USGS
science for a changing world

Recd
11/22/99

GEOMORPHIC AND SEDIMENTOLOGIC CHARACTERISTICS OF ALLUVIAL REACHES IN THE BLACK CANYON OF THE GUNNISON NATIONAL MONUMENT, COLORADO

Water-Resources Investigations Report 99–4082

U.S. Department of the Interior
U.S. Geological Survey

Prepared in cooperation with the
NATIONAL PARK SERVICE

Geomorphic and Sedimentologic Characteristics of Alluvial Reaches in the Black Canyon of the Gunnison National Monument, Colorado

By John G. Elliott *and* Lauren A. Hammack

U.S. GEOLOGICAL SURVEY

Water-Resources Investigations Report 99–4082

Prepared in cooperation with the
NATIONAL PARK SERVICE

Denver, Colorado
1999

U.S. DEPARTMENT OF THE INTERIOR
BRUCE BABBITT, Secretary

U.S. GEOLOGICAL SURVEY
Charles G. Groat, Director

For additional information write to:

District Chief
U.S. Geological Survey
Box 25046, Mail Stop 415
Denver Federal Center
Denver, CO 80225-0046

Copies of this report can be purchased from:

U.S. Geological Survey
Information Services
Box 25286
Federal Center
Denver, CO 80225

CONTENTS

FIGURES

TABLES

CONVERSION FACTORS, VERTICAL DATUM, AND ABBREVIATIONS

Multiply	By	To obtain
millimeter (mm)	0.03937	inch
foot (ft)	0.3048	meter (m)
mile (mi)	1.609	kilometer (km)
square foot (ft^2)	0.0929	square meter
square mile (mi^2	2.590	square kilometer
acre-foot (acre-ft)	0.001233	cubic hectometer
foot per second (ft/s)	0.3048	meter per second
cubic foot per second (ft^3/s)	0.02832	cubic meter per second
pound per square foot (lb/ft^2)	4.882	kilogram per square meter
pound per square foot (lb/ft^2)	47.88	newton per square meter
pound per cubic foot (lb/ft^3)	157.1	newton per cubic meter (N/m^3)

Sea level: In this report, "sea level" refers to the National Geodetic Vertical Datum of 1929 (NGVD of 1929)—a geodetic datum derived from a general adjustment of the first-order level nets of both the United States and Canada, formerly called Sea Level Datum of 1929.

Geomorphic and Sedimentologic Characteristics of Alluvial Reaches in the Black Canyon of the Gunnison National Monument, Colorado

By John G. Elliott *and* Lauren A. Hammack[1]

ABSTRACT

The Black Canyon of the Gunnison River in western Colorado includes several alluvial reaches that are potentially sensitive to changes in streamflow. Sediment derived from talus slopes, rockfall, and tributary debris flows periodically is reworked and redeposited on the streambed, streambanks, and alternate bars in these alluvial reaches, providing a growth medium for riparian vegetation. Geomorphic and sedimentologic data were collected and evaluated at two alluvial reaches in the Black Canyon—Warner Point and Red Rock Canyon. These data and the hydrologic data from an upstream gaging station were used to calculate the entrainment potential of a large range of sediment sizes on a variety of fluvial geomorphic surfaces typical of the Gunnison River in the Black Canyon and other canyon rivers.

The HEC-2 and HEC-RAS one-dimensional water-surface profiles models were used to estimate water-surface elevations, flow depths, and hydraulic conditions for discharges from 2,000 to 20,000 cubic feet per second at surveyed channel cross sections in the two study reaches. A peak discharge of 9,470 cubic feet per second in 1995 and onsite observations and photographs in 1994 and 1995 confirmed sediment entrainment or reworking on several geomorphic surfaces inundated by the peak discharge. Physical evidence of sediment entrainment, or absence of sediment entrainment, on inundated sediment-measurement sites generally was consistent with critical shear stresses estimated with a dimensionless critical shear stress, τ^*_c, of 0.030 in the Warner Point study reach. Sediment-entrainment potential over a range of discharges was summarized by the ratio of boundary shear stress to the critical shear stress (τ_o/τ_c), given local hydraulic geometry and sediment-size characteristics. Differing entrainment potential for similar geomorphic surfaces indicates that estimation of minimum streamflow requirements based on sediment mobility requires site-specific geomorphic and sedimentologic data.

INTRODUCTION

The Black Canyon of the Gunnison River is noted for its gorge-like characteristics, which include expansive views, precipitous bedrock cliffs, and a cascading river (Hansen, 1965; Warner and Walker, 1972). However, several reaches of the river through the Black Canyon of the Gunnison National Monument (BLCA) exhibit characteristics of an alluvial river: fluvially deposited banks and bars, riffle-pool channel geometry, and a riparian ecosystem. Although the large-scale features of canyon rivers, such as the Gunnison River in the Black Canyon, are influenced by regional geology, the channel and riparian zone of many canyon river reaches are dominated by fluvial processes. Geomorphic and botanical conditions in the alluvial reaches of canyon rivers are controlled both by the characteristics of fluvially deposited sediment and the hydraulics of flood discharges. Consequently, changes in streamflow can produce adverse effects in canyon rivers similar to those in alluvial rivers (Elliott and Hammack, in press).

[1]National Park Service, Fort Collins, Colorado.

Purpose and Scope

This report summarizes geomorphic, hydraulic, and sedimentologic data collected in two alluvial reaches of BLCA in 1990, 1994, and 1995 and hydrologic data recorded since the early 20th century. The geomorphic and sedimentologic data were collected and evaluated by the U.S. Geological Survey (USGS) in cooperation with the National Park Service (NPS). The objective of this study was to determine the hydraulic conditions and minimum streamflow necessary to entrain, or initiate the movement of, the sediment median-particle size (d_{50}) of the alluvial streambanks and bars in selected areas of BLCA vulnerable to encroachment by riparian vegetation. The data and these findings will be used by the NPS to assess the sensitivity of the riparian corridor in BLCA to potential changes in the Gunnison River streamflow regime.

The hydrologic data are from streamflow-gaging station 09128000 Gunnison River below Gunnison Tunnel, located at the eastern end of BLCA (fig. 1). This gage, operated by the USGS, has recorded peak discharge since 1906 and continuous streamflow since 1911. Geomorphic data include channel geometry characteristics determined from onsite surveys made with a total-station laser theodolite and sediment-size distributions. Hydraulic data include flow depths and boundary shear stresses at several channel cross sections reconstructed from one-dimensional, water-surface profiles modeling. Sedimentologic data include particle-size analyses of streambanks, alluvial bars, and a tributary debris-flow deposit. Estimates of sediment-entrainment potential were based on the sediment critical shear stress and modeled hydraulic conditions at several locations on the cross sections.

Acknowledgments

The study was made possible with the support of the National Park Service and the cooperation of the Bureau of Reclamation. Mark Wondzell (NPS) established and surveyed several cross sections in 1990 that were subsequently relocated and resurveyed by the authors. In addition, Mark Wondzell organized logistical support, assisted in all field-data collection efforts, and provided critical oversight of methodology and reviews of the early drafts of this report.

The authors are especially grateful to Myron Chase (NPS) and George Ingersoll (USGS) for their dedication, invaluable logistical support, and assistance in the field. Greg Auble, Jonathan Friedman, and Mike Scott (USGS) contributed critical insight and discussion concerning the sensitivity of riparian vegetation to hydrologic variability. Additional field assistance was provided by Michelle DeLong, Chris Gable, and Erica Van Wie (NPS) and by Randy Parker and Erik Eggleston (USGS). Technical reviews of the report were provided by David F. Meyer and Mark E. Smith (USGS).

STUDY AREA

The area generally known as the Black Canyon of the Gunnison River includes the Black Canyon of the Gunnison National Monument (BLCA), the Gunnison Gorge, and reaches now inundated by Blue Mesa, Morrow Point, and Crystal Reservoirs (fig. 1). This study was limited to the BLCA portion of the Black Canyon.

Geologic Setting

The geology of the Black Canyon area exerts a strong influence on the Gunnison River canyon and fluvial geomorphology in BLCA. Incision of the Gunnison River into folded and faulted areas of the Gunnison uplift has exposed predominantly Precambrian igneous and metamorphic rocks at river level (Hansen, 1965), but variations in the structure and lithology give rise to a variety of canyon and fluvial morphologies. Sediment transported by the river is supplied by local talus slopes and rockfall and by debris flows from ephemeral tributaries (Elliott and Parker, 1997).

Riparian Zone Characteristics

The Black Canyon riparian zone can be classified into general reach categories determined by the dominant physical processes affecting river morphology and sediment characteristics. The two most common reach categories are talus/rockfall and alluvial. A third reach category, debris flow, is less common although significant geomorphically because of the large volume of mixed-size sediment delivered

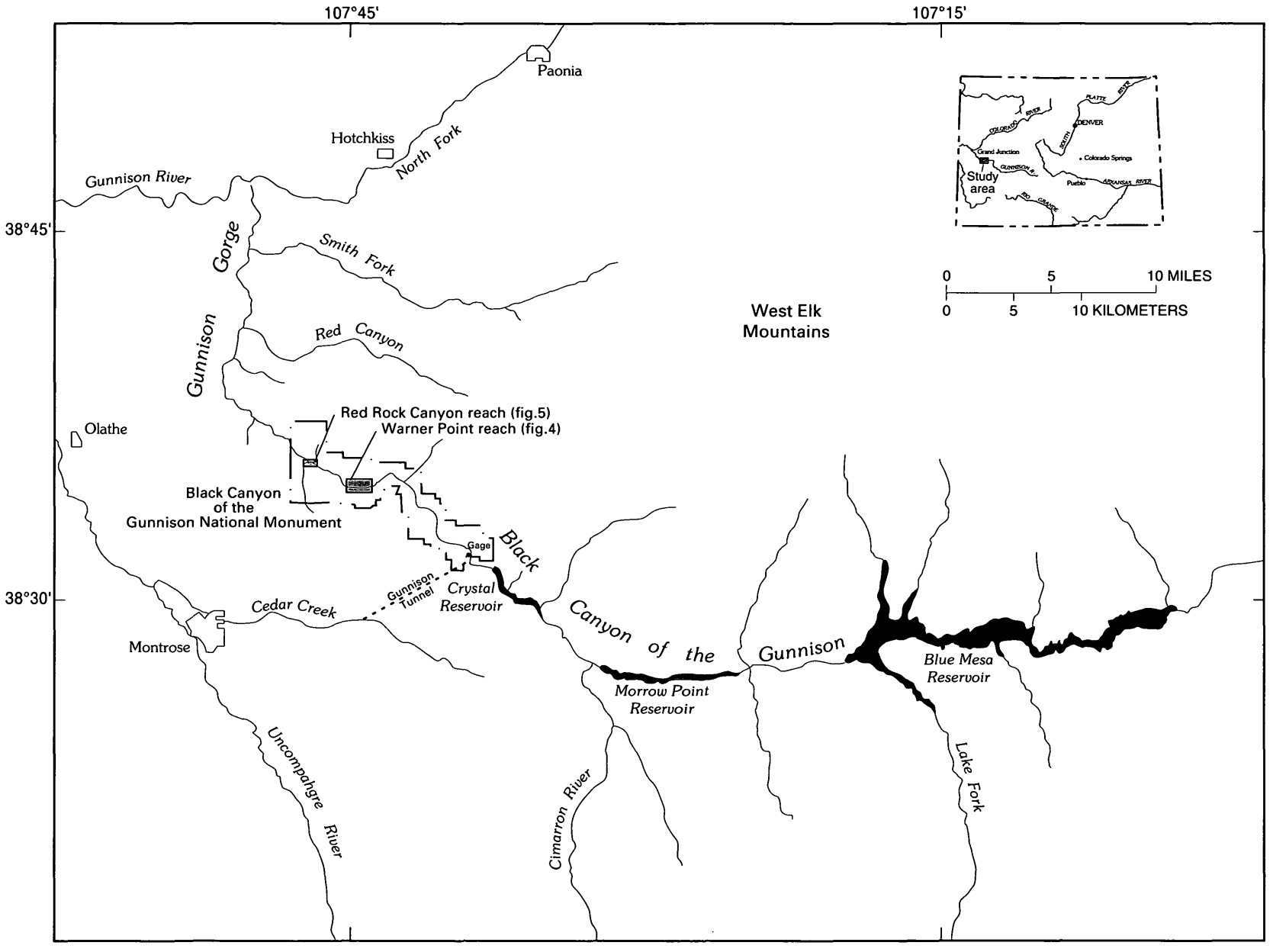

Figure 1. Map of the Gunnison River and the Black Canyon of the Gunnison National Monument, Colorado.

to the river. Debris flows from ephemeral tributaries occur intermittently in both talus/rockfall and alluvial reaches of BLCA.

Talus/rockfall reaches have steep river gradients and very narrow canyon floors bordered by steep talus or colluvial slopes and sheer bedrock cliffs. The streambed and banks in these reaches are composed of a high proportion of large, angular rock fragments that have fallen directly into the channel and generally remain there. These reaches have limited, if any, deposits of finer grain, fluvially deposited sediments where riparian plant communities can develop. Talus/rockfall is the predominant reach category in BLCA; photographic interpretation indicates that the riparian zone in these reaches has changed very little since 1939.

In other river reaches in BLCA, substantial portions of the channel bed and banks are composed of fluvially transported and deposited sand, gravel, cobbles, and boulders. These are alluvial reaches. Streambanks composed of well-rounded gravel and cobbles are more prominent in these reaches than in talus/rockfall reaches, and fluvially deposited bars can be as much as several tens of feet wide (fig. 2). Alluvial deposits of notable size are present in the upper and lower reaches of BLCA but generally are absent between river mile (RM) 4.6 upstream from The Narrows and RM 7.1 upstream from The Painted Wall where the river gradient is very steep (fig. 3). River miles in this report are expressed as the downstream distance measured from the Gunnison Tunnel diversion in the eastern part of BLCA (fig. 1).

The Gunnison River profile (fig. 3) over a 13-mile segment from the Gunnison Tunnel Diversion to the western boundary of BLCA (fig. 1) was derived from USGS 1:24,000 topographic maps with 20- and 40-foot contour intervals. Superimposed on the river profile in figure 3 is a graph showing the percentage of the river reach between adjacent contour crossings bounded by alluvial deposits. Aerial-photograph interpretation indicates that approximately 35 percent of the Gunnison River in BLCA is bordered on one or both banks by alluvial sedimentary deposits.

The greater abundance of fluvial sediments deposited in alluvial reaches provides a growth medium for riparian vegetation and the gravel- and cobble-size bed material that is critical for some aquatic biota. Alluvial reaches, in contrast to talus/rockfall reaches, are areas dominated by streamflow-dependent processes, including intermittent sediment transport, storage, and remobilization. Consequently, the fluvial geomorphology, riparian vegetation, and bed-material composition in alluvial reaches are more sensitive to streamflow-regime modification caused by climate change or anthropogenic activity. Some alluvial reaches have exhibited noticeable geomorphic and vegetation changes since the first aerial photographs were taken of BLCA in 1939.

Two alluvial reaches of BLCA were studied. The Warner Point study reach (fig. 4) extended from RM 8.1 to RM 8.7, and the Red Rock Canyon study reach (fig. 5) extended from RM 10.9 to 11.4 (fig. 3). Talus/rockfall reaches were not included in this study because of their relative insensitivity to streamflow-regime modification.

Hydrology

The Gunnison River Basin has a drainage area of almost 8,000 mi^2 at its confluence with the Colorado River at Grand Junction, Colorado, and contributes 42 percent of the Colorado River annual streamflow at the Colorado/Utah State line. Most of the main-stem runoff is generated by spring snowmelt; however, convective and monsoonal summer storms generate runoff in ephemeral tributaries in the lower parts of the watershed (Elliott and Parker, 1992).

Four major reservoirs and one transbasin diversion affect streamflow entering the Black Canyon. Blue Mesa Reservoir, completed in October 1965, Morrow Point Reservoir (1968), and Crystal Reservoir (1977) comprise the Wayne N. Aspinall Unit, a group of three large reservoirs in the central part of the Gunnison River Basin just upstream from BLCA (fig. 1). The three reservoirs of the Aspinall Unit have a combined storage capacity of about 52 percent of the average annual streamflow of the Gunnison River. Diversion and impoundment before water year 1966 had relatively little effect on the flood hydrology of the Black Canyon. Impoundment by Blue Mesa Reservoir has had a substantial effect on the downstream flow regime; therefore, the postregulation period for the purpose of this study is defined as 1966 to the present (Elliott and Parker, 1997).

The USGS streamflow-gaging station 09128000, Gunnison River below Gunnison Tunnel, has recorded peak discharge since 1906 and continuous discharge since 1911. The gage is located approximately 2.3 miles downstream from Crystal

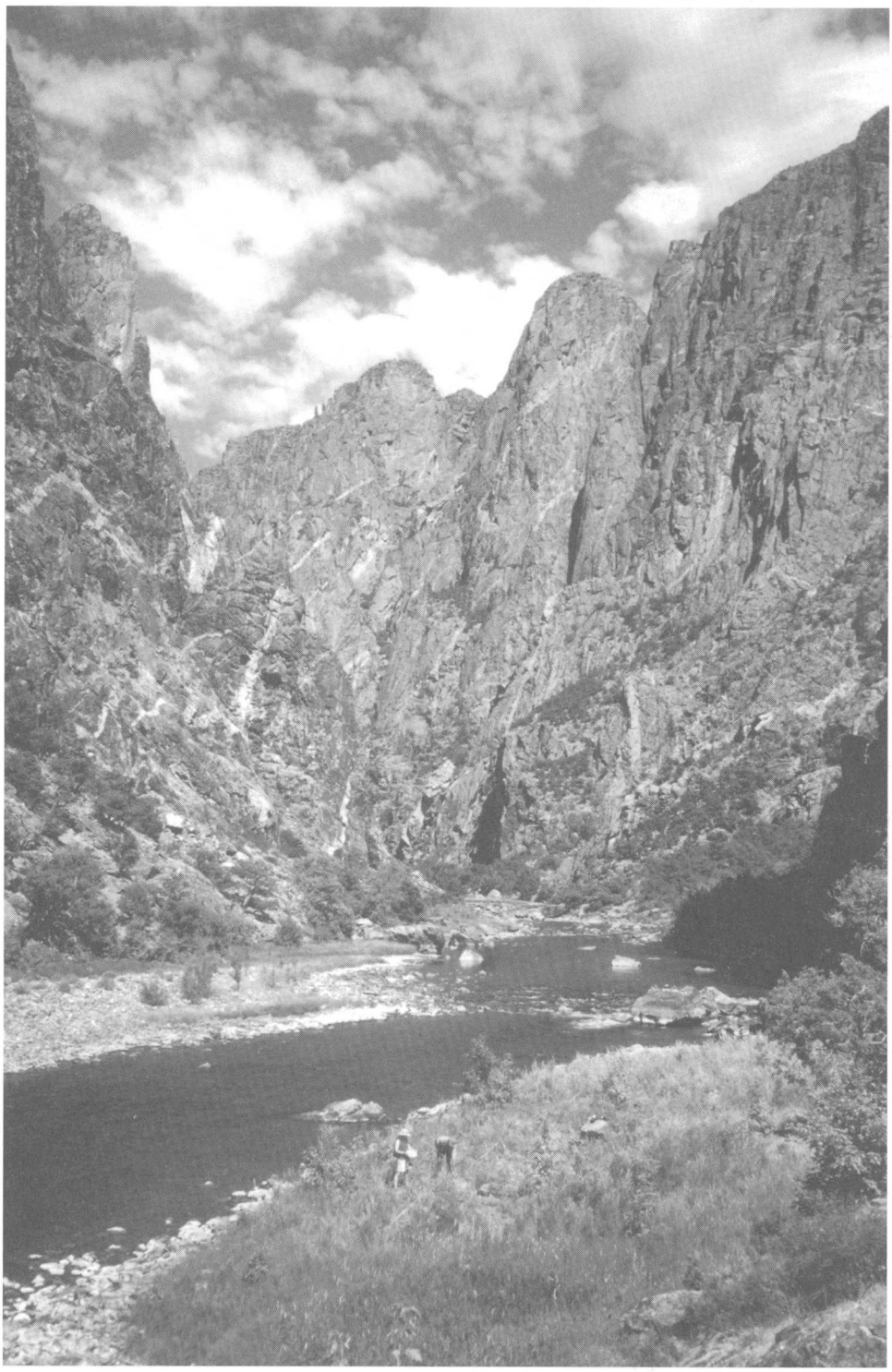

Figure 2. Photograph showing fluvially deposited bars in the upper part of the Warner Point study reach. Photograph taken from monument location 0004 (see fig. 4), July 31, 1994; discharge was approximately 300 cubic feet per second.

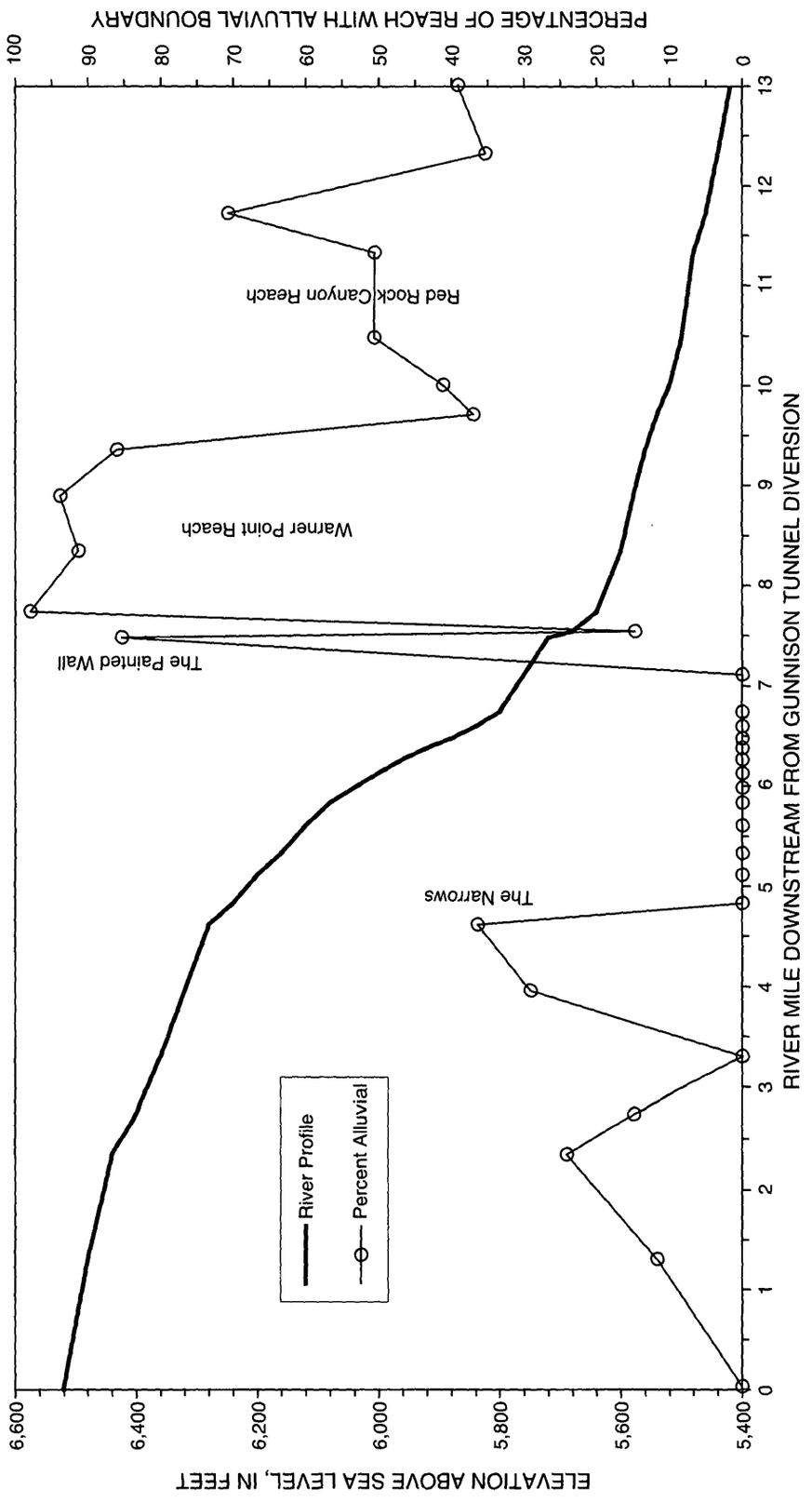

Figure 3. Gunnison River profile and the location and relative abundance of alluvial deposits in Black Canyon of the Gunnison National Monument.

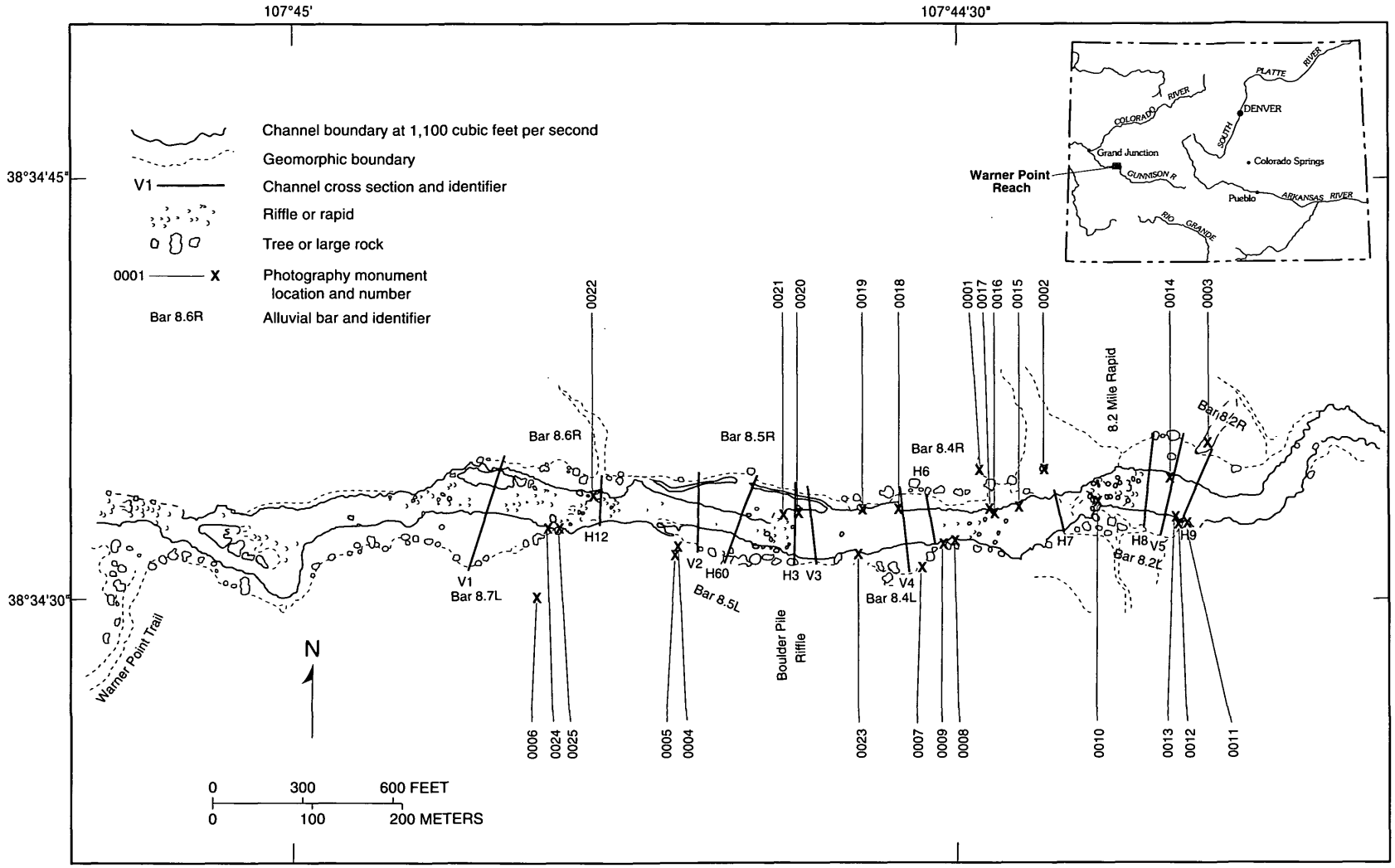

Figure 4. Map of the Warner Point study reach showing location of surveyed cross sections and oblique-photography monuments. Channel boundary at 1,100 cubic feet per second determined from June 27, 1982, aerial photograph.

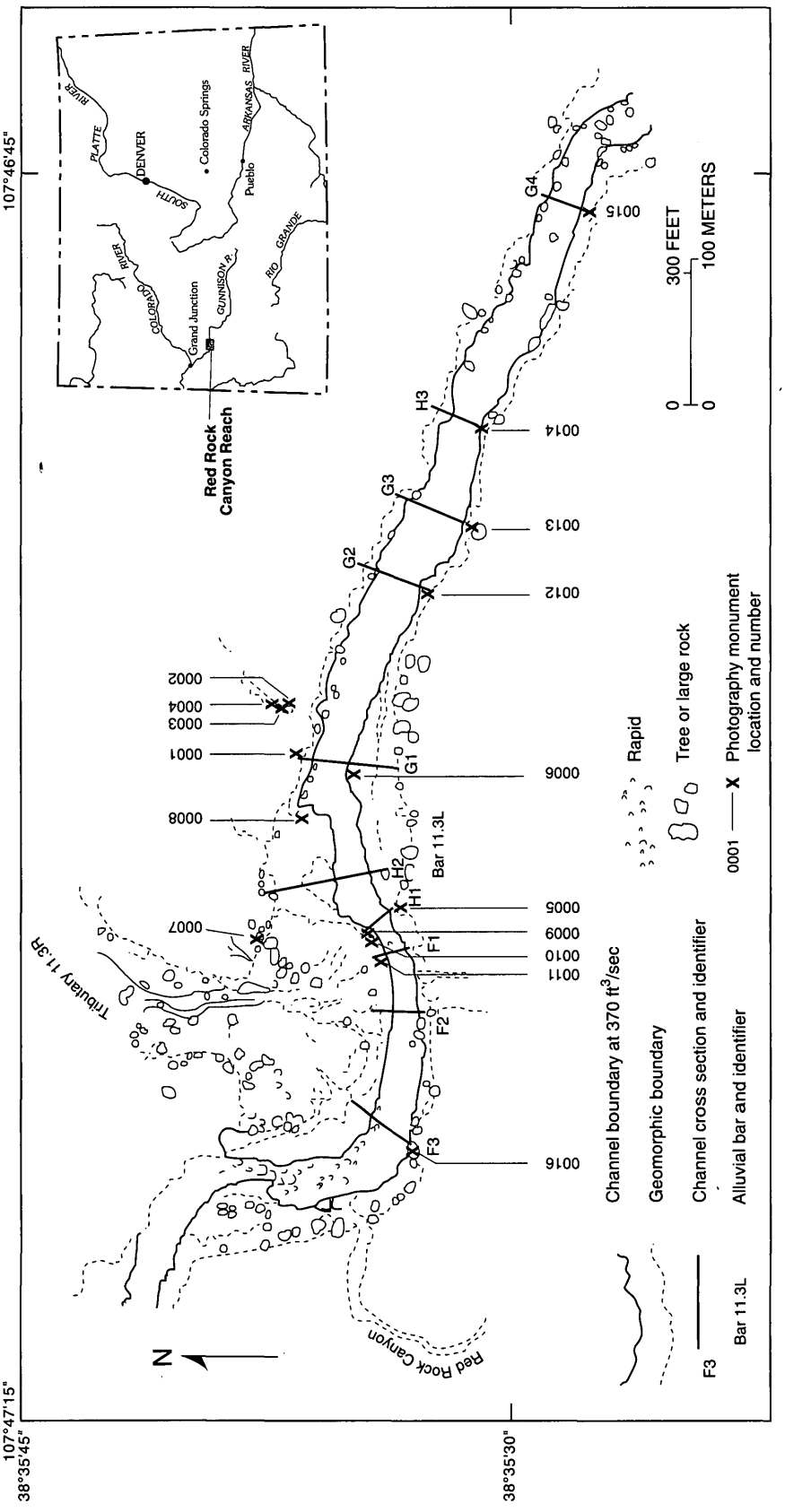

Figure 5. Map of the Red Rock Canyon study reach showing location of surveyed cross sections and oblique-photography monuments. Channel boundary at 370 cubic feet per second determined from July 3, 1989, aerial photograph.

Dam (the downstream-most of the Aspinall Unit dams), about 0.4 mile downstream from the Gunnison Tunnel (fig. 1), and 8.2 miles upstream from the beginning of the Warner Point study reach. The Gunnison Tunnel diverts as much as approximately 1,000 ft^3/s for irrigation from April through October. The nonconsumed portion of the diverted water eventually is returned to the Gunnison River by way of the Uncompahgre River and does not pass through the Black Canyon. The drainage area upstream from the gage is 3,965 mi^2. Discharge data from 1911 through 1994 were used to determine magnitude-frequency relations and flow-duration characteristics for periods before (preregulation) and after (postregulation) reservoir construction.

Upstream reservoirs have altered the timing and magnitude of Gunnison River flood peaks since 1966; however, the mean annual discharge in the Black Canyon (954,000 acre-feet) has not changed since about 1930. Monthly mean discharge during the snowmelt season (April through July) has decreased 63 percent since reservoir regulation, whereas monthly mean discharge for the remainder of the year (August through March) has increased 170 percent (Elliott and Parker, 1992). Flood magnitudes of given recurrence intervals (RI) have decreased substantially since 1966. Recurrence intervals, the reciprocal of the probability that a specific discharge will be equaled or exceeded in any given year, were determined according to methods prescribed by the U.S. Interagency Advisory Committee on Water Data (1982). The 10-year flood decreased from 14,900 to 7,000 ft^3/s, the 5-year flood from 12,700 to 5,460 ft^3/s, and the mean annual flood from 9,290 to 4,040 ft^3/s. While reservoir operation has attenuated flood peaks in the Black Canyon, it also has augmented moderate streamflows. The duration of daily mean streamflows between 1,140 and 3,000 ft^3/s has increased from an average of 12 percent of the time, or an average of about 44 days per year from 1911 to 1965, to 38 percent of the time, or an average of about 139 days per year from 1966 to 1994 (Elliott and Parker, 1997). Recurrence intervals and streamflow durations of selected discharges in the preregulation and postregulation periods are summarized in table 1.

GEOMORPHIC AND SEDIMENTOLOGIC CHARACTERISTICS

Geomorphic and sedimentologic data were collected and evaluated at two alluvial reaches in the BLCA. These data and the hydrologic data from the upstream gaging station were used to calculate the entrainment potential of a large range of sediment sizes on a variety of fluvial geomorphic surfaces typical of the Gunnison River in the Black Canyon and other canyon rivers.

Aerial Photography

Aerial and oblique photography have been used to document changes in geomorphology and riparian conditions by several investigators (Webb, 1996; Webb and others, 1996; Elliott and Hammack, in press). Aerial photography was used to identify alluvial and talus/rockfall reaches of BLCA and to evaluate changes in alluvial deposits, debris-flow deposits, and riparian vegetation through time. Black and white, natural color, and color/infrared images covering part or all of BLCA have been made intermittently since 1939. Most of these photographs were made in the late summer or early autumn and facilitate comparison of fluvial features at relatively low discharges. Years of photography used in this study are 1939, 1950, 1954, 1966, 1976, 1982, 1989, and 1992. An index of most of these aerial photographs is available from the USGS Earth Science Information Center in Denver, Colorado.

Monumented Oblique Photography

Oblique photographs were taken of the study reaches, monumented cross sections, alluvial bars, and sediment-sampling sites and can be used to document future changes in alluvial features if they occur. Photographs of the BLCA study reaches were made from monumented vantage points at river level to at least 100 feet above the river level to show different perspectives of the Gunnison River. Several changes in riparian vegetation and sediment deposits in the two study reaches were observed and photographed between 1994 and 1995 and confirm sediment entrainment at several locations (Elliott and Hammack, in press). Monumented photography locations and numbers are shown in figures 4 and 5 and are listed in

Table 1. Streamflow characteristics for the Gunnison River downstream from the Gunnison Tunnel, U.S. Geological streamflow-gaging station 09128000

[Recurrence interval, in years, equals reciprocal of exceedance probability, calculated with annual instantaneous discharge peak; streamflow duration in percentage of time specific discharge is equaled or exceeded calculated with daily mean discharge; ft^3/s, cubic foot per second; %, percentage]

Discharge (ft^3/s)	Recurrence interval		Streamflow duration	
	Pre-regulation 1911–65 (years)	Post-regulation 1966–94 (years)	Pre-regulation 1911–65 (% time)	Post-regulation 1966–94 (% time)
300			80	80
500			51	65
1,000		1.01	28	47
1,140		1.02	26	42
2,000		1.18	19	17
2,200	1.01	1.25	18	12
3,000	1.04	1.65	14	4.0
4,000	1.09	2.5	11	1.2
5,000	1.17	4.0	7.9	0.72
5,140	1.18	4.2	7.5	0.70
6,000	1.30	6.0	5.8	0.60
7,000	1.50	10	4.1	0.46
8,000	1.70	16	2.8	0.28
9,000	2.0	24	1.9	0.13
10,000	2.5	35	1.2	0.03
11,000	3.2	50	0.8	
12,000	4.4	75	0.5	
13,000	6.0	100	0.3	
14,000	8.0		0.16	
15,000	11		0.09	
16,000	16			
17,000	24			
18,000	35			
19,000	55			
20,000	90			

table 2. A complete set of photographs taken from these locations is in the possession of the NPS Water Resources Division in Fort Collins, Colorado, and selected photographs are presented in the appendix at the end of this report.

Geomorphic Surveys

Surveys were made of the study reaches with a total-station laser theodolite to quantify geomorphic features, high-water elevations, channel cross-section characteristics, and river gradient. Data from these surveys also were used as input to one-dimensional, water-surface profile models and sediment-entrainment potential calculations. The Warner Point study reach (fig. 4) was approximately 3,000 ft long and was surveyed in 1990, 1994, and 1995. Twelve channel cross sections were surveyed in the Warner Point reach and were used to calibrate the one-dimensional, water-surface profile model. Hydraulic-geometry characteristics and sediment-entrainment potential were calculated at 8 of the 12 cross sections. Geomorphic features surveyed included streambanks, alluvial bars, and overflow channels between the bars and adjacent talus slopes.

Table 2. Locations of oblique-photography monuments in the Warner Point and Red Rock Canyon study reaches, Black Canyon of the Gunnison National Monument

[L and R, left and right river sides from a downstream-viewed orientation; river mileage measured from Gunnison Tunnel Diversion; XS, cross section; N, north; E, east; S, south; W, west; LWS and RWS, left and right water surface at discharge of 300-400 cubic feet per second; LEW and REW, left and right edge of water at discharge of 300-400 feet per second; upst, upstream; dnst, downstream; ~, approximately; Hub and number, location of the total-station laser theodolite for geomorphic surveys]

Monument number	Monument location	Principal subjects	Orientations	Remarks
		Warner Point Reach		
0001	Base of cliff at R talus slope	8.2 Mile Rapid, XS-H6, XS-V4	SE,S,SW	~300 ft upst from XS-V4, ~60 ft above RWS.
0002	Boulder in R talus slope	XS-5, 8.2 Mile Rapid, XS-V4	E,S,SW	Near XS-H7, ~35 ft above RWS.
0003	Outcrop above Bar 8.2R	Bar 8.2R, XS-H9, XS-V5	SE,S,SW	Near XS-H9, ~40 ft above Bar 8.2R.
0004	Slope above Bar 8.5L	Bars 8.5L, 8.5R, XS-V2	NE,E	~10 ft downslope from trail, ~100 ft above LWS.
0005	Slope above Bar 8.5L	Bars 8.6R, 8.5L, 8.5R, XS-V2	W,NW,NE,E	~50 ft upslope from trail, ~160 ft above LWS.
0006	Outcrop above Bar 8.7L	Bar 8.7L, XS-V1	NW,N,NE	~300 ft above LWS and E end of Bar 8.7L.
0007	Outcrop above Bar 8.4L	Bars 8.5R, 8.4R, XS-V2, H3, V3, V4	W,NW,NE,E	~150 ft above LWS and E end of Bar 8.4L.
0008	Boulder on L bank	Bar 8.4L, XS-V4	W	Near XS-H6, ~10 ft S of LEW.
0009	Boulder on L bank	Bar 8.4L, XS-V4	W	Near XS-H6, ~10 ft S of LEW.
0010	Large boulder 8.2 Mile Rapid	XS-H7	W	On L side of 8.2 Mile Rapid.
0011	Outcrop above Bar 8.2L	Bars 8.2L, 8.2R	W,NW,NE	Near XS-H9, ~40 ft above and ~20 ft S of LEW.
0012	Boulder on L bank	Bar 8.2L, XS-V5	W	At L end XS-H9 and 1 ft above LWS.
0013	Boulder on L bank	Bar 8.2L, XS-V5	W	Near L end XS-H9 and 1.5 ft above LWS.
0014	Boulder on R bank	Bar 8.2R, XS-V5 and H9	W, E	At XS-V5 near REW.
0015	Boulder on R bank	Bar 8.4R	E,W	~160 ft dnst from XS-H7, 4 ft above RWS.
0016	Large boulder on R bank	Bar 8.4R	E,W	~220 ft upst from XS-H6, 10 ft above RWS.
0017	Boulder on Bar 8.4R	Bar 8.4R	E,W	~200 ft upst from XS-H6, ~25 ft N of REW.
0018	Large boulder on R bank	Bar 8.4R, XS-V4 and H6	E	Near XS-V4, ~12 ft above RWS.
0019	Large boulder on R bank	XS-V3 and V4	W,E	~180 ft upst from XS-V3, ~15 ft above RWS.
0020	Boulder on R bank	Bar 8.5R, XS-H3, XS-V3	W,E	At XS-H3.
0021	Boulder on R bank	Bar 8.5R, XS-V3, H3, and H60	E,SW,W,NW	~50 ft dnst from XS-H3, ~2 ft above RWS.
0022	Large boulder on R bank	XS-H12, Bar 8.7L, Bar 8.6R	E,SW,W,NW	~30 ft dnst from XS-H12.
0023	Large boulder on L bank	Bars 8.4R and 8.4L, XS-V4	NE, E	~180 ft dnst from XS-V4, ~10 ft above LWS.
0024	Boulder on L bank	Bar 8.7L, Bar 8.6R, XS-V1	W, NW, E	~200 ft upst from XS-V1, ~ 4 ft above LWS.
0025	Outcrop above L bank	Bar 8.7L	W	~100 ft above LWS near high trail.

Table 2. Locations of oblique-photography monuments in the Warner Point and Red Rock Canyon study reaches, Black Canyon of the Gunnison National Monument—Continued

[L and R, left and right river sides from a downstream-viewed orientation; river mileage measured from Gunnison Tunnel Diversion; XS, cross section; N, north; E, east; S, south; W, west; LWS and RWS, left and right water surface at discharge of 300-400 cubic feet per second; LEW and REW, left and right edge of water at discharge of 300-400 feet per second; upst, upstream; dnst, downstream; ~, approximately; Hub and number, location of the total-station laser theodolite for geomorphic surveys]

Monument number	Monument location	Principal subjects	Orientations	Remarks
		Red Rock Canyon Reach		
0001	R colluvial slope	Bar 11.3L, Fan 11.3R	S, SW, W	At R headpin on XS-G1, ~50 ft N of REW.
0002	Outcrop above R bank	XS-G2, G3, and G4	SE	~100 ft above Hub1 and RM-2, upst from XS-G1.
0003	Outcrop above R bank	XS-G1 and H2, Bar 11.3L	S, SW	~100 ft above Hub1 and RM-2, upst from XS-G1.
0004	Outcrop above R bank	Bar 11.3L, XS-G1, H2 and H1	SW, W	~100 ft above Hub1 and RM-2, upst from XS-G1.
0005	Outcrop above L bank	Debris Fan 11.3R	NW, N, NE	~100 ft above L headpin of XS-H1.
0006	Boulder on Bar 11.3L	Bar 11.3L	SE, N, W	~50 ft dnst from XS-G1.
0007	Boulder on Debris Fan 11.3R	Debris Fan 11.3R	SE,S,SW,W	At Hub3, 2 ft N of large boulder on fan head.
0008	Boulder on R bank	R boulder bar, XS-H2	W	Midway between XS-G1 and H2.
0009	Boulder on Debris Fan 11.3R	Debris Fan 11.3R distal margin	E, W	15 ft dnst from XS-F1 at REW.
0010	Boulder on Debris Fan 11.3R	Debris Fan 11.3R distal margin	E, W	67 ft dnst from XS-F1, 2 ft above REW.
0011	Boulder on Debris Fan 11.3R	Debris Fan 11.3R distal margin	E, W	10 ft dnst from XS-F2, 3 ft south of REW.
0012	Large boulder on L bank	L bank at XS-G2	NW, SE	Near XS-G2, LEW.
0013	L colluvial slope	XS-G3	NE	At L headpin on XS-G3.
0014	Large boulder on L bank	L bank at XS-H3	NW, NE, SE	At RM5 on XS-H3.
0015	L colluvial slope	L bank at XS-G4	NW, NE, E	At L headpin on XS-G4.
0016	Outcrop on L bank	Rapid at Debris Fan 11.3R	N, NE, E	Near L headpin of XS-F3 on foot trail.

The Red Rock Canyon study reach (fig. 5) was approximately 2,300 ft long and was surveyed in 1994; selected cross sections were resurveyed in 1995. Ten channel cross sections were surveyed in the Red Rock Canyon reach and were used to calibrate the one-dimensional, water-surface profiles model. Hydraulic-geometry characteristics were calculated at 6 of the 10 cross sections, and sediment-entrainment potential was calculated at 4 cross sections. Geomorphic features surveyed included streambanks, alluvial bars, and the distal margin of a tributary debris fan.

Sediment-Size Analysis

Sediment-size characteristics, including the median particle size (d_{50}), were determined for a variety of surfaces deemed geomorphically distinct and (or) botanically significant using the Wolman (1954) method. These surfaces included the streambed and streambanks, the lateral and top surfaces of large alluvial bars, and the distal margin of a debris-flow deposit (tables 3 and 4). The streambed and low-flow channel of most cross sections in the study reaches are composed of material in the large cobble- and boulder-size range; however, streambanks and alluvial bars are composed of finer material in the gravel-, cobble-, and occasionally boulder-size range. Most of the initial sediment measurements were made in 1994; however, a few sites were first measured in 1995. Replicate measurements were made in 1995 at several sites initially measured in 1994 to determine the effect of the 1995 peak discharge (9,470 ft^3/s) on sediment-size characteristics. Subsurface sediment size was not determined except for the left bank at cross section V4 in the Warner Point study reach, where the ratio of surface d_{50} (47 mm) to subsurface d_{50} (20 mm) was 2.35, within the range stated by Parker and others (1982) as typical for streams having gravel and cobble beds.

One-Dimensional Streamflow Modeling

The one-dimensional water-surface profiles model HEC-2 (Hydrologic Engineering Center, 1990) was used to estimate water-surface elevations, flow depths, and hydraulic conditions through the study reaches for a range of discharges from 2,000 to 20,000 ft^3/s. The model used surveyed channel cross sections and was calibrated with observed water-surface elevations and high-water marks associated with discharges of 336, 614, 766, 1,024, 1,584, 3,450, 5,170, 6,800, and 9,400 ft^3/s in the Warner Point reach. HEC-RAS (Hydrologic Engineering Center, 1997) was used to model the Red Rock Canyon reach. This model was calibrated using discharges of 400, 1,000, 2,310, and 3,170 ft^3/s. Discharges at the Warner Point and Red Rock Canyon reaches were assumed to be comparable to discharges recorded a few hours earlier at USGS gaging station 09128000 upstream.

The hydraulic models were calibrated by varying the Manning's n roughness coefficient until the calculated water-surface elevations matched the surveyed water-surface elevations as closely as possible. Calculated water-surface elevations were within 0.2 to 0.5 ft of the surveyed elevations for most calibration discharges, having differences less than 10 percent of the calculated flow depth for a specific discharge. Although the Manning's n roughness coefficient was used as a calibration tool, reasonable values for each cross section were maintained based on estimated values from Barnes (1967) and Arcement and Schneider (1989).

Computational errors were minimized, and the accuracy of the models was improved by inserting interpolated cross sections to balance velocity heads and water-surface elevations. Additionally, multiple friction loss equations were evaluated, and conveyance ratios were kept within tolerances where possible and were otherwise determined acceptable. Hydraulic output from the modeling runs included water-surface elevations and energy gradients, from which flow depths and boundary shear stresses at specific locations on the cross sections were calculated. Tables 5 and 6 summarize hydraulic-geometry characteristics in the study reaches for simulated discharges.

Shear Stress Distribution

Sediment entrainment in stream channels is partly a function of the boundary shear stress acting on sediment particles resting on or in the streambed or other inundated alluvial surfaces. Shear stress is proportional to the square of streamflow velocity and is most accurately determined by measurements of velocity vectors in downstream, lateral, and vertical directions. When velocity data are unavailable, mean shear stress in a channel cross section commonly is

Table 3. Sediment-size statistics and critical shear stress for the median particle size, Warner Point study reach

[Station, sample location on cross section from left endpoint; Percentile, percentile of the size distribution; lc, sampled across the entire low-flow channel; ns, not sampled or not calculated; Critical shear for the median sediment size calculated with equation 2; Shields parameter is variable depending on pavement and subsurface properties; ft, foot; mm, millimeters; lb/ft^2, pound per square foot]

Cross section	Sample year	Sample code	Station (ft)	16th Percentile (mm)	50th Percentile (mm)	84th Percentile (mm)	Maximum particle size (mm)	Critical shear with Shields parameter 0.030 (lb/ft^2)	Critical shear with Shields parameter 0.045 (lb/ft^2)	Remarks
V1	1994	XChan	lc	90	230	420	1,450	2.33	3.50	Sampled from station 196 to 358.
V1	1994	LBldBar	138	60	130	300	700	1.32	1.98	
V1	1994	LBank	198	105	240	400	660	2.43	3.65	
V1	1994	RBldBar	287.5	50	180	370	750	1.82	2.74	Sampled near right edge of water.
V2	ns	XChan	ns	ns	ns	ns	740	ns	ns	Low-flow channel not sampled.
V2	1994	LBldBar	66	160	270	400	600	2.74	4.11	
V2	1994	LBank	81	100	212	450	600	2.15	3.22	
V2	1994	RBank	161	80	125	190	280	1.27	1.90	
V2	1994	RSlope	168	55	98	170	380	0.99	1.49	Midway up bar slope.
V2	1994	RBldBar	186	50	125	200	400	1.27	1.90	
V2	1994	ROvrFlo	228	31	140	210	400	1.42	2.13	
V2	1995	LBank	80	34	128	224	410	1.30	1.95	
V2	1995	RBank	161	46	98	145	520	0.99	1.49	
V2	1995	RSlope	168	52	100	158	225	1.01	1.52	
H60	ns	XChan	ns	ns	ns	ns	ns	ns	ns	Low-flow channel not sampled.
H60	1994	LBank	87	25	130	390	700	1.32	1.98	
H60	1995	RBank	172	55	180	333	820	1.82	2.74	
H60	1995	RBldBar	192	65	172	472	670	1.74	2.62	
H3	ns	XChan	ns	ns	ns	ns	ns	ns	ns	Low-flow channel not sampled.
H3	1994	RBank	195	18	90	185	1,000	0.91	1.37	Sample overlaps both V3 and H3.
H3	1995	RBank	196	49	110	191	1,240	1.12	1.67	Sample overlaps both V3 and H3.
V3	1994	XChan	lc	5	150	310	500	1.52	2.28	Sampled from station 42 to 205.
V3	1994	LBank	44	2	14	67	370	0.14	0.21	Gravel in backwater of Boulder Pile Riffle.
V3	1994	RBank	203	18	90	185	1,000	0.91	1.37	Sample overlaps both V3 and H3.
V3	1994	RBldBar	211	ns	ns	ns	320	0.00	0.00	
V3	1995	LBar	21	41	80	149	2,410	0.81	1.22	

Table 3. Sediment-size statistics and critical shear stress for the median particle size, Warner Point study reach—Continued

[Station, sample location on cross section from left endpoint; Percentile, percentile of the size distribution; lc, sampled across the entire low-flow channel; ns, not sampled or not calculated; Critical shear for the median sediment size calculated with equation 2; Shields parameter is variable depending on pavement and subsurface properties; ft, foot; mm, millimeters; lb/ft^2, pound per square foot]

Cross section	Sample year	Sample code	Station (ft)	16th Percentile (mm)	50th Percentile (mm)	84th Percentile (mm)	Maximum particle size (mm)	Critical shear with Shields parameter 0.030 (lb/ft^2)	Critical shear with Shields parameter 0.045 (lb/ft^2)	Remarks
V3	1995	RBank	204	49	110	191	1,240	1.12	1.67	Sample overlaps both V3 and H3.
V3	1995	ROvrFlo	241	8	40	76	760	0.41	0.61	
V4	1994	XChan	lc	100	270	680	830	2.74	4.11	Sampled from station 79 to 205.
V4	1994	LGrsTer	75	2	9	22	92			
V4	1994	LCblBar	81	2	20	48	101	0.20	0.30	Subsurface sample, 300-mm-deep pit.
V4	1994	LBank	85	22	47	118	490	0.48	0.71	
V4	1994	RCblBar	203	32	72	165	900	0.73	1.09	
V4	1994	ROvrFlo	235	17	87	245	580	0.88	1.32	
V4	1995	LBank	80	2	38	97	470	0.39	0.58	
V4	1995	ROvrFlo	243	39	170	320	1,000	1.72	2.59	
H6	1994	REddy	162	9	16	23	38	0.16	0.24	Gravel deposited in 1993 behind large boulder.
H6	1995	REddy	162	15	58	162	300	0.59	0.88	
H7	1994	LBank	24	ns	ns	ns	900	0.00	0.00	
H8	1995	ROvrFlo	283	10	25	42	60	0.25	0.38	
V5	1994	XChan	lc	70	250	410	550	2.53	3.80	Sampled from station 75 to 219.
V5	1994	LSplay	56	35	55	74	205	0.56	0.84	
V5	1994	LBank	80	128	220	350	530	2.23	3.35	
V5	1994	RBank	216	38	145	300	550	1.47	2.20	
V5	1994	RGvlTer	273	14	32	52	120	0.32	0.49	Downstream from Box Elder number 132.
V5	1994	RPtBar	277	26	64	105	500	0.65	0.97	
V5	1995	LBar	61	2	160	306	455	1.62	2.43	
V5	1995	RPtBar	275	11	50	110	430	0.51	0.76	
H9	ns	XChan	ns	ns	ns	ns	ns	ns	ns	Low-flow channel not sampled.
H9	1994	LBank	86	128	220	350	530	2.23	3.35	Sampled at V5.
H9	1994	RBank	216	38	145	300	550	1.47	2.20	Sampled at V5.
H9	1994	RPtBar	277	26	64	105	500	0.65	0.97	Sampled at V5
H9	1995	RPtBar	275	11	50	110	430	0.51	0.76	Sampled at V5.

Table 4. Sediment-size statistics and critical shear stress for the median particle size, Red Rock Canyon study reach

[Station, sample location on cross section from left endpoint; Percentile, percentile of the size distribution; lc, sampled across the entire low-flow channel; Critical shear for the median sediment size calculated with Equation 2; Shields parameter is variable depending on pavement and subsurface properties; ft, foot; mm, millimeters; lb/ft^2, pound per square foot; DF, debris flow]

Cross section	Sample year	Sample code	Station (ft)	16th Percentile (mm)	50th Percentile (mm)	84th Percentile (mm)	Maximum particle size (mm)	Critical shear with Shields parameter 0.030 (lb/ft^2)	Critical shear with Shields parameter 0.045 (lb/ft^2)	Remarks
F2	1994	RBank	85	43	165	500	1,000	1.67	2.51	DF-2 deposit near distal fan margin.
F1	1994	RBank	78	43	165	500	1,000	1.67	2.51	DF-2 deposit near distal fan margin.
H1	1994	RBank	90	13	50	174	500	0.51	0.76	DF-3 deposit near distal fan margin.
H1	1994	Fan	105	11	33	109	320	0.33	0.50	DF-3 deposit on fan.
H2	1994	RBldBar	181	79	320	450	650	3.24	4.87	Reworked boulders from debris fan.
G1	1994	XChan	lc	11	64	168	600	0.65	0.97	Sampled from station 52 to 210.
G1	1994	LBldBar	45	2	100	250	1,050	1.01	1.52	Sand covers boulders many places.
G1	1994	LGvlBar	79	16	36	76	120	0.36	0.55	Well sorted gravels.
G2	1994	XChan	lc	51	90	250	900	0.91	1.37	Sampled from station 38 to 142.

approximated by the relation between boundary shear stress, flow depth, and energy gradient, given by the duBoys equation (Chow, 1959, p. 168):

$$\tau_0 = \gamma D S \qquad (1)$$

where τ_0 is the mean boundary shear stress, in pounds per square foot;

γ is the specific weight of water (62.4 pounds per cubic foot);

D is the mean flow depth, in feet; and

S is the energy gradient, in foot per foot, for a specific discharge.

Assumptions for using equation 1 are (1) the channel cross section has a regular, or trapezoidal, shape and width at least 10 times greater than its depth, (2) streamflow is steady (there is a continuity of discharge from cross section to cross section in the reach), and (3) streamflow is uniform (velocity is constant in both magnitude and direction through the reach). Application of equation 1 is inappropriate in channel sections where there is a strong lateral variation in acceleration or where abrupt, local changes in streambed gradient occur. Cross sections in this study were not trapezoidal, although all had single-thread channels at less than flood discharges; all had width at least 20 times mean flow depth, and many were approximately symmetrical at less than flood discharges. Streamflow in the Warner Point and Red Rock Canyon study reaches was assumed to be steady; there were no significant local inflows to either reach, and infiltration losses were assumed to be insignificant.

Most natural streams do not completely satisfy the assumptions for equation 1, and the boundary shear stress associated with any specific discharge is

Table 5. Modeled hydraulic geometry of Warner Point study reach cross sections

[Water surface, energy gradient, channel area, and channel top width from HEC-2 model; ft^3/s, cubic foot per second; ft, foot; ft/ft, foot per foot; ft^2, square foot; ft/s, foot per second; lb/ft^2, pound per square foot]

Reference discharge (ft^3/s)	Water-surface elevation (ft)	Energy gradient (ft/ft)	Channel area (ft^2)	Channel top width (ft))	Mean flow depth (ft)	Mean flow velocity (ft/s)	Mean bed shear (lb/ft^2)
			Cross Section V1				
2,000	516.13	0.0074	474.16	172.08	2.76	4.22	1.27
2,250	516.38	0.0073	515.64	173.48	2.97	4.36	1.35
3,000	517.06	0.0071	629.70	177.18	3.55	4.76	1.57
4,000	517.85	0.0068	766.99	181.53	4.23	5.22	1.79
5,000	518.56	0.0066	891.10	185.37	4.81	5.61	1.98
6,000	519.20	0.0063	1,007.46	188.90	5.33	5.96	2.10
7,000	519.79	0.0060	1,122.26	194.52	5.77	6.24	2.16
8,000	520.34	0.0058	1,486.43	295.65	5.03	5.38	1.82
9,000	520.87	0.0055	1,644.28	312.93	5.25	5.47	1.80
9,500	521.12	0.0054	1,724.30	321.44	5.36	5.51	1.81
10,000	521.36	0.0052	1,804.31	329.94	5.47	5.54	1.77
11,000	521.84	0.0050	1,975.69	354.63	5.57	5.57	1.74
15,000	523.56	0.0040	2,648.91	361.25	7.33	5.66	1.83
20,000	525.43	0.0029	3,453.61	368.12	9.38	5.79	1.70
			Cross Section V2				
2,000	522.31	0.0046	347.26	93.30	3.72	5.76	1.07
2,250	522.58	0.0046	415.46	98.14	4.23	5.42	1.22
3,000	523.30	0.0044	446.48	100.26	4.45	6.72	1.22
4,000	524.14	0.0043	664.06	181.75	3.65	6.02	0.98
5,000	524.88	0.0041	789.65	191.86	4.12	6.33	1.05
6,000	525.56	0.0040	915.89	202.75	4.52	6.55	1.13
7,000	526.18	0.0038	1,040.40	212.45	4.90	6.73	1.16
8,000	526.77	0.0037	1,172.21	228.82	5.12	6.82	1.18
9,000	527.32	0.0035	1,298.52	232.26	5.59	6.93	1.22
9,500	527.58	0.0035	1,361.52	233.94	5.82	6.98	1.27
10,000	527.84	0.0034	1,424.23	235.62	6.04	7.02	1.28
11,000	528.34	0.0033	1,550.58	238.87	6.49	7.09	1.34
15,000	530.15	0.0029	2,023.84	250.26	8.09	7.41	1.46
20,000	532.11	0.0025	2,573.10	258.94	9.94	7.77	1.55

Table 5. Modeled hydraulic geometry of Warner Point study reach cross sections—Continued

[Water surface, energy gradient, channel area, and channel top width from HEC-2 model; ft^3/s, cubic foot per second; ft, foot; ft/ft, foot per foot; ft^2, square foot; ft/s, foot per second; lb/ft^2, pound per square foot]

Reference discharge (ft^3/s)	Water-surface elevation (ft)	Energy gradient (ft/ft)	Channel area (ft^2)	Channel top width (ft))	Mean flow depth (ft)	Mean flow velocity (ft/s)	Mean bed shear (lb/ft^2)
			Cross Section H60				
2,000	522.98	0.0036	414.63	125.80	3.30	4.82	0.74
2,250	523.24	0.0035	427.98	127.34	3.36	5.26	0.73
3,000	523.97	0.0032	561.26	157.42	3.57	5.35	0.71
4,000	524.80	0.0030	720.03	198.90	3.62	5.56	0.68
5,000	525.54	0.0028	860.76	214.14	4.02	5.81	0.70
6,000	526.22	0.0026	1,001.23	229.52	4.36	5.99	0.71
7,000	526.83	0.0025	1,141.06	244.49	4.67	6.13	0.73
8,000	527.41	0.0024	1,287.87	265.34	4.85	6.21	0.73
9,000	527.95	0.0023	1,431.68	270.52	5.29	6.29	0.76
9,500	528.21	0.0022	1,503.33	272.50	5.52	6.32	0.76
10,000	528.47	0.0022	1,574.98	274.48	5.74	6.35	0.79
11,000	528.96	0.0021	1,718.19	278.20	6.18	6.40	0.81
15,000	530.72	0.0018	2,276.19	304.61	7.47	6.59	0.84
20,000	532.64	0.0016	2,935.08	307.16	9.56	6.81	0.95
			Cross Section H3				
2,000	525.67	0.0033	586.17	232.60	2.52	3.41	0.52
2,250	525.86	0.0034	639.45	236.66	2.70	3.52	0.57
3,000	526.39	0.0034	732.22	240.74	3.04	4.10	0.65
4,000	527.03	0.0035	882.05	243.53	3.62	4.53	0.79
5,000	527.59	0.0036	1,013.85	245.96	4.12	4.93	0.93
6,000	528.12	0.0036	1,134.82	248.17	4.57	5.29	1.03
7,000	528.61	0.0036	1,248.88	250.23	4.99	5.61	1.12
8,000	529.07	0.0037	1,358.74	252.20	5.39	5.89	1.24
9,000	529.50	0.0037	1,468.30	253.24	5.80	6.13	1.34
9,500	529.71	0.0037	1,520.33	253.38	6.00	6.25	1.39
10,000	529.92	0.0037	1,572.36	253.52	6.20	6.36	1.43
11,000	530.32	0.0036	1,676.63	253.80	6.61	6.56	1.48
15,000	531.80	0.0034	2,079.30	254.88	8.16	7.21	1.73
20,000	533.43	0.0029	2,574.69	258.12	9.97	7.77	1.81

Table 5. Modeled hydraulic geometry of Warner Point study reach cross sections—Continued

[Water surface, energy gradient, channel area, and channel top width from HEC-2 model; ft^3/s, cubic foot per second; ft, foot; ft/ft, foot per foot; ft^2, square foot; ft/s, foot per second; lb/ft^2, pound per square foot]

Reference discharge (ft^3/s)	Water-surface elevation (ft)	Energy gradient (ft/ft)	Channel area (ft^2)	Channel top width (ft))	Mean flow depth (ft)	Mean flow velocity (ft/s)	Mean bed shear (lb/ft^2)
			Cross Section V3				
2,000	525.97	0.0014	699.45	222.31	3.15	2.86	0.27
2,250	526.17	0.0014	735.06	224.67	3.27	3.06	0.29
3,000	526.54	0.0015	825.20	230.16	3.59	3.64	0.34
4,000	527.36	0.0017	974.69	237.95	4.10	4.10	0.43
5,000	527.94	0.0018	1,104.04	244.50	4.52	4.53	0.51
6,000	528.47	0.0019	1,226.20	248.64	4.93	4.89	0.58
7,000	528.97	0.0020	1,342.19	252.97	5.31	5.22	0.66
8,000	529.44	0.0021	1,454.88	257.88	5.64	5.50	0.74
9,000	529.88	0.0022	1,567.59	262.41	5.97	5.74	0.82
9,500	530.09	0.0022	1,622.03	264.33	6.14	5.86	0.84
10,000	530.30	0.0022	1,676.47	266.25	6.30	5.96	0.86
11,000	530.70	0.0022	1,786.62	270.08	6.62	6.16	0.91
15,000	532.17	0.0022	2,218.27	273.46	8.11	6.76	1.11
20,000	533.79	0.0019	2,750.42	275.69	9.98	7.27	1.18
			Cross Section V4				
2,000	526.48	0.0026	512.31	188.02	2.72	3.90	0.44
2,250	526.69	0.0026	551.66	191.40	2.88	4.08	0.47
3,000	527.26	0.0026	580.86	194.75	2.98	5.16	0.48
4,000	527.93	0.0027	717.28	239.58	2.99	5.58	0.50
5,000	528.52	0.0027	854.27	247.75	3.45	5.85	0.58
6,000	529.05	0.0027	983.85	255.66	3.85	6.10	0.65
7,000	529.55	0.0027	1,108.22	264.56	4.19	6.32	0.71
8,000	530.01	0.0027	1,228.60	266.96	4.60	6.51	0.78
9,000	530.45	0.0027	1,345.87	268.81	5.01	6.69	0.84
9,500	530.66	0.0027	1,401.98	269.68	5.20	6.78	0.88
10,000	530.86	0.0027	1,458.08	270.56	5.39	6.86	0.91
11,000	531.25	0.0027	1,569.17	272.28	5.76	7.01	0.97
15,000	532.68	0.0025	1,998.77	278.85	7.17	7.50	1.12
20,000	534.23	0.0021	2,535.83	291.06	8.71	7.89	1.14

Table 5. Modeled hydraulic geometry of Warner Point study reach cross sections—Continued

[Water surface, energy gradient, channel area, and channel top width from HEC-2 model; ft^3/s, cubic foot per second; ft, foot; ft/ft, foot per foot; ft^2, square foot; ft/s, foot per second; lb/ft^2, pound per square foot]

Reference discharge (ft^3/s)	Water-surface elevation (ft)	Energy gradient (ft/ft)	Channel area (ft^2)	Channel top width (ft))	Mean flow depth (ft)	Mean flow velocity (ft/s)	Mean bed shear (lb/ft^2)
			Cross Section V5				
2,000	542.55	0.0073	510.88	170.64	2.99	3.91	1.36
2,250	542.74	0.0073	524.28	174.51	3.00	4.29	1.37
3,000	543.27	0.0074	598.94	198.05	3.02	5.01	1.40
4,000	543.89	0.0075	734.25	235.42	3.12	5.45	1.46
5,000	544.44	0.0075	871.46	274.07	3.18	5.74	1.49
6,000	544.93	0.0076	1,009.07	303.00	3.33	5.95	1.58
7,000	545.38	0.0076	1,143.82	322.46	3.55	6.12	1.68
8,000	545.81	0.0076	1,279.94	333.86	3.83	6.25	1.82
9,000	546.21	0.0076	1,409.90	335.62	4.20	6.38	1.99
9,500	546.40	0.0075	1,474.48	336.50	4.38	6.44	2.05
10,000	546.58	0.0075	1,539.06	337.37	4.56	6.50	2.13
11,000	546.94	0.0075	1,664.72	339.06	4.91	6.61	2.30
15,000	548.25	0.0069	2,142.43	345.41	6.20	7.00	2.67
20,000	549.65	0.0057	2,695.69	351.53	7.67	7.42	2.73
			Cross Section H9				
2,000	543.14	0.0039	584.92	156.47	3.74	3.42	0.91
2,250	543.34	0.0040	626.60	186.35	3.36	3.59	0.84
3,000	543.90	0.0042	713.86	213.72	3.34	4.20	0.88
4,000	544.54	0.0045	861.83	223.48	3.86	4.64	1.08
5,000	545.09	0.0048	995.00	256.56	3.88	5.03	1.16
6,000	545.60	0.0050	1,131.99	291.01	3.89	5.30	1.21
7,000	546.06	0.0053	1,260.01	294.92	4.27	5.56	1.41
8,000	546.49	0.0054	1,378.45	296.49	4.65	5.80	1.57
9,000	546.89	0.0056	1,488.91	297.95	5.00	6.04	1.75
9,500	547.08	0.0057	1,542.39	298.65	5.16	6.16	1.84
10,000	547.27	0.0058	1,595.87	299.35	5.33	6.27	1.93
11,000	547.63	0.0059	1,699.04	300.70	5.65	6.47	2.08
15,000	548.92	0.0061	2,087.78	305.72	6.83	7.18	2.60
20,000	550.30	0.0058	2,553.72	311.63	8.19	7.83	2.97

Table 6. Modeled hydraulic geometry of Red Rock Canyon study reach cross sections

[Water surface, energy gradient, channel area, and channel top width from HEC-2 model; ft^3/s, cubic foot per second; ft, foot; ft/ft, foot per foot; ft^2, square foot; ft/s, foot per second; lb/ft^2, pound per square foot]

Reference discharge (ft^3/s)	Water surface elevation (ft)	Energy gradient (ft/ft)	Channel area (ft^2)	Channel top width (ft)	Mean flow depth (ft)	Mean flow velocity (ft/s)	Mean bed shear (lb/ft^2)
			Cross Section F2				
2,000	4,993.45	0.00973	328.05	69.60	4.71	6.10	2.86
2,200	4,993.67	0.01019	343.94	70.63	4.87	6.40	3.10
3,000	4,994.49	0.01177	402.90	74.27	5.42	7.45	3.98
4,000	4,995.33	0.01347	466.92	78.17	5.97	8.57	5.02
5,000	4,996.04	0.01503	523.95	82.04	6.39	9.54	5.99
6,000	4,996.62	0.01675	572.49	85.20	6.72	10.48	7.02
7,000	4,997.14	0.01836	617.43	87.40	7.06	11.34	8.09
8,000	4,997.60	0.01995	658.15	88.68	7.42	12.16	9.24
9,000	4,998.02	0.02135	695.14	89.79	7.74	12.95	10.31
9,500	4,998.22	0.02210	712.99	90.32	7.89	13.32	10.89
10,000	4,998.41	0.02282	730.51	90.84	8.04	13.69	11.45
11,000	4,998.77	0.02432	762.97	91.79	8.31	14.42	12.62
15,000	4,999.90	0.03098	868.75	94.81	9.16	17.27	17.71
20,000	5,002.44	0.02646	1,118.42	102.26	10.94	17.88	18.06
			Cross Section F1				
2,000	4,994.40	0.0144	209.60	53.82	3.89	9.54	3.51
2,200	4,994.63	0.0148	222.47	55.54	4.01	9.89	3.69
3,000	4,995.48	0.0158	271.83	61.67	4.41	11.04	4.33
4,000	4,996.42	0.0162	333.12	68.53	4.86	12.01	4.91
5,000	4,997.52	0.0143	413.24	78.18	5.29	12.10	4.71
6,000	4,998.39	0.0135	487.74	90.01	5.42	12.30	4.58
7,000	4,999.13	0.0132	556.13	93.55	5.94	12.59	4.90
8,000	4,999.93	0.0123	631.20	95.38	6.62	12.67	5.10
9,000	5,000.45	0.0128	687.29	107.01	6.42	13.09	5.13
9,500	5,001.10	0.0111	759.94	113.78	6.68	12.50	4.65
10,000	5,001.64	0.0102	821.80	119.12	6.90	12.17	4.39
11,000	5,003.07	0.0075	1,003.05	133.56	7.51	10.97	3.53
15,000	5,005.81	0.0060	1,403.42	153.52	9.14	10.69	3.39
20,000	5,008.33	0.0053	1,792.93	155.00	11.57	11.15	3.82

Table 6. Modeled hydraulic geometry of Red Rock Canyon study reach cross sections—Continued

[Water surface, energy gradient, channel area, and channel top width from HEC-2 model; ft^3/s, cubic foot per second; ft, foot; ft/ft, foot per foot; ft^2, square foot; ft/s, foot per second; lb/ft^2, pound per square foot]

Reference discharge (ft^3/s)	Water surface elevation (ft)	Energy gradient (ft/ft)	Channel area (ft^2)	Channel top width (ft)	Mean flow depth (ft)	Mean flow velocity (ft/s)	Mean bed shear (lb/ft^2)
			Cross Section H1				
2,000	4,995.81	0.0023	366.93	81.29	4.51	5.45	0.65
2,200	4,996.17	0.0023	396.58	83.71	4.74	5.55	0.67
3,000	4,997.48	0.0020	520.27	98.80	5.27	5.77	0.65
4,000	4,998.88	0.0017	662.00	103.47	6.40	6.04	0.69
5,000	5,000.01	0.0016	781.03	111.17	7.03	6.40	0.72
6,000	5,000.97	0.0016	896.25	127.65	7.02	6.69	0.70
7,000	5,001.84	0.0016	1,012.80	139.65	7.25	6.91	0.71
8,000	5,002.61	0.0015	1,124.78	150.28	7.48	7.11	0.72
9,000	5,003.40	0.0015	1,248.44	161.21	7.74	7.21	0.72
9,500	5,003.73	0.0015	1,302.48	165.78	7.86	7.29	0.72
10,000	5,004.08	0.0015	1,361.22	169.56	8.03	7.35	0.73
11,000	5,004.91	0.0014	1,504.38	177.81	8.46	7.31	0.71
15,000	5,007.38	0.0012	1,974.52	203.19	9.72	7.60	0.74
20,000	5,009.89	0.0011	2,518.79	230.20	10.94	7.94	0.77
			Cross Section H2				
2,000	4,996.41	0.00032	634.59	202.00	3.14	3.15	0.06
2,200	4,996.79	0.00029	715.30	220.77	3.24	3.08	0.06
3,000	4,998.16	0.00018	1,024.49	231.46	4.43	2.93	0.05
4,000	4,999.58	0.00013	1,364.44	250.86	5.44	2.93	0.05
5,000	5,000.76	0.00011	1,676.27	283.22	5.92	2.98	0.04
6,000	5,001.78	0.00010	1,976.86	300.81	6.57	3.04	0.04
7,000	5,002.70	0.00009	2,258.51	307.65	7.34	3.10	0.04
8,000	5,003.53	0.00009	2,514.76	312.07	8.06	3.18	0.04
9,000	5,004.35	0.00008	2,772.67	315.47	8.79	3.25	0.04
9,500	5,004.70	0.00008	2,884.72	316.69	9.11	3.29	0.04
10,000	5,005.06	0.00008	2,999.37	317.93	9.43	3.33	0.05
11,000	5,005.87	0.00007	3,257.59	320.94	10.15	3.38	0.05
15,000	5,008.39	0.00007	4,079.59	332.96	12.25	3.68	0.05
20,000	5,010.94	0.00007	4,945.28	345.16	14.33	4.04	0.06

Table 6. Modeled hydraulic geometry of Red Rock Canyon study reach cross sections—Continued

[Water surface, energy gradient, channel area, and channel top width from HEC-2 model; ft^3/s, cubic foot per second; ft, foot; ft/ft, foot per foot; ft^2, square foot; ft/s, foot per second; lb/ft^2, pound per square foot]

Reference discharge (ft^3/s)	Water surface elevation (ft)	Energy gradient (ft/ft)	Channel area (ft^2)	Channel top width (ft)	Mean flow depth (ft)	Mean flow velocity (ft/s)	Mean bed shear (lb/ft^2)
			Cross Section G1				
2,000	4,996.24	0.00072	370.51	133.80	2.77	5.40	0.12
2,200	4,996.62	0.00057	422.14	144.06	2.93	5.21	0.10
3,000	4,997.90	0.00026	625.26	164.86	3.79	4.80	0.06
4,000	4,999.26	0.00015	854.63	173.30	4.93	4.68	0.05
5,000	5,000.39	0.00011	1,054.96	180.27	5.85	4.74	0.04
6,000	5,001.38	0.00009	1,239.40	191.09	6.49	4.84	0.04
7,000	5,002.29	0.00008	1,414.37	196.71	7.19	4.95	0.04
8,000	5,003.09	0.00008	1,574.38	201.71	7.81	5.08	0.04
9,000	5,003.89	0.00007	1,738.35	206.27	8.43	5.18	0.04
9,500	5,004.23	0.00007	1,809.14	207.37	8.72	5.25	0.04
10,000	5,004.59	0.00007	1,882.25	208.49	9.03	5.31	0.04
11,000	5,005.39	0.00006	2,050.11	211.02	9.72	5.37	0.04
15,000	5,007.82	0.00006	2,572.93	219.92	11.70	5.83	0.04
20,000	5,010.27	0.00006	3,125.64	231.77	13.49	6.40	0.05
			Cross Section G2				
2,000	4,996.78	0.00057	448.82	117.09	3.83	4.46	0.14
2,200	4,997.09	0.00054	486.52	120.12	4.05	4.52	0.14
3,000	4,998.33	0.00044	640.14	127.94	5.00	4.69	0.14
4,000	4,999.68	0.00038	820.81	141.36	5.81	4.87	0.14
5,000	5,000.82	0.00035	988.68	153.51	6.44	5.06	0.14
6,000	5,001.80	0.00034	1,143.98	163.20	7.01	5.24	0.15
7,000	5,002.69	0.00033	1,293.25	170.67	7.58	5.41	0.16
8,000	5,003.49	0.00032	1,431.38	174.71	8.19	5.59	0.17
9,000	5,004.28	0.00032	1,578.37	185.83	8.49	5.70	0.17
9,500	5,004.63	0.00032	1,642.67	188.86	8.70	5.78	0.17
10,000	5,004.98	0.00032	1,709.24	191.94	8.91	5.85	0.18
11,000	5,005.76	0.00031	1,862.76	198.87	9.37	5.91	0.18
15,000	5,008.20	0.00031	2,374.70	220.42	10.77	6.32	0.21
20,000	5,010.68	0.00032	2,945.96	240.30	12.26	6.79	0.24

nonuniformly distributed across the channel. Lateral and downstream variations in cross-section morphology and variations in energy gradient with discharge result in a wide range of boundary shear stresses and, consequently, produce variable conditions for sediment entrainment, sorting, and deposition. Point depths along each cross section were substituted for the cross-section mean flow depth in equation 1 to examine the relative effects of different discharges at a variety of locations within the study reaches. Shear stresses associated with a range of discharges from 2,000 to 20,000 ft^3/s were calculated at intervals on each cross section by using output from the HEC-2 and HEC-RAS models. Cross-section geometry and the variation in cross-channel shear-stress distribution at three reference discharges are shown in figures 6 and 7.

Sediment Entrainment

Breakup and entrainment of the relatively coarse streambed surface, or pavement, in a gravel/cobble stream periodically is necessary to adjust or maintain channel dimensions and to entrain the underlying gravel, sand, silt, and clay (Milhous, 1982). It also appears that encroaching riparian vegetation can be temporarily eradicated when the median particle size (d_{50}) of sediment in alluvial banks and bars are regularly entrained (Friedman and Auble, in press). The primary objective of this study was to determine the hydraulic conditions and minimum streamflow necessary to entrain sediment d_{50} of the alluvial banks and bars in selected areas of BLCA vulnerable to riparian vegetation encroachment.

The critical shear stress (τ_c), the shear stress at which general movement of sediment begins, has been related to sediment-size characteristics (Shields, 1936; Lane, 1955; Fahnestock, 1963; Carling, 1983; Komar, 1987; Wilcock, 1992). Elliott and Parker (1997) and J.G. Elliott and L.A. Hammack (written commun., 1999) used the Shields (1936) equation to estimate the critical shear stress for entrainment of sediment d_{50}:

$$\tau_c = \tau^*_c (\gamma_s - \gamma) d_{50} \qquad (2)$$

where τ_c is the critical shear stress, in newtons per square meter;

τ^*_c is the dimensionless critical shear stress or Shields parameter;

γ_s is the specific weight of sediment (assumed to be 25,990 N/m^3);

γ is the specific weight of water (9,807 N/m^3); and

d_{50} is the median particle size, in meters.

Critical shear stress in equation 2 (newtons per square meter) is converted to English units (pounds per square foot) by multiplying by 0.02088.

Once τ_c has been identified for a specific deposit, the critical discharge, the minimum streamflow required to entrain sediment d_{50}, can be estimated by equating τ_o with τ_c and using the relation between shear stress and discharge at a specific cross-section location.

Wilcock (1992, p. 297) states that equation 2 and d_{50} can be used to provide a minimum estimate of the shear stress necessary to initiate general movement of a mixed-size sediment based on experiments using sediments with d_{50} up to about 20 mm. Lane's (1955) data indicate that the Shields equation is applicable for sediments with a 75th percentile (d_{75}) up to about 100 mm. When the boundary shear stress, τ_o, is compared with the critical shear stress, τ_c, for the d_{50} at various locations on the cross sections, it is possible to evaluate the sediment-entrainment potential of each discharge with respect to a particular geomorphic surface or location on a cross section (figs. 6 and 7).

The critical shear stress associated with sediment entrainment (eq. 2) is, at best, a minimum estimate of the critical discharge because only a small area of the entire surface or a few particles of the d_{50} size may be entrained by the critical discharge (Lisle and others, 1993; Milhous, 1982). Wilcock and McArdell (1993) observed that complete mobilization of a size fraction, such as d_{50}, occurred at roughly twice the shear stress necessary for incipient motion of individual particles in that size fraction.

Use of equation 2 requires an estimated or calculated dimensionless critical shear stress, or Shields parameter, τ^*_c. Neill (1968) recommended a τ^*_c of 0.030 for streambeds composed of coarse materials; however, other investigators have demonstrated a variable τ^*_c in channels with mixed-size sediments (Komar, 1987) and in channels where the bed-surface size is significantly larger than the subsurface size (Parker and others, 1982; Andrews, 1983). Powell and Ashworth (1995) found τ^*_c varied with the strength of bed-surface structure. Tightly structured beds (those

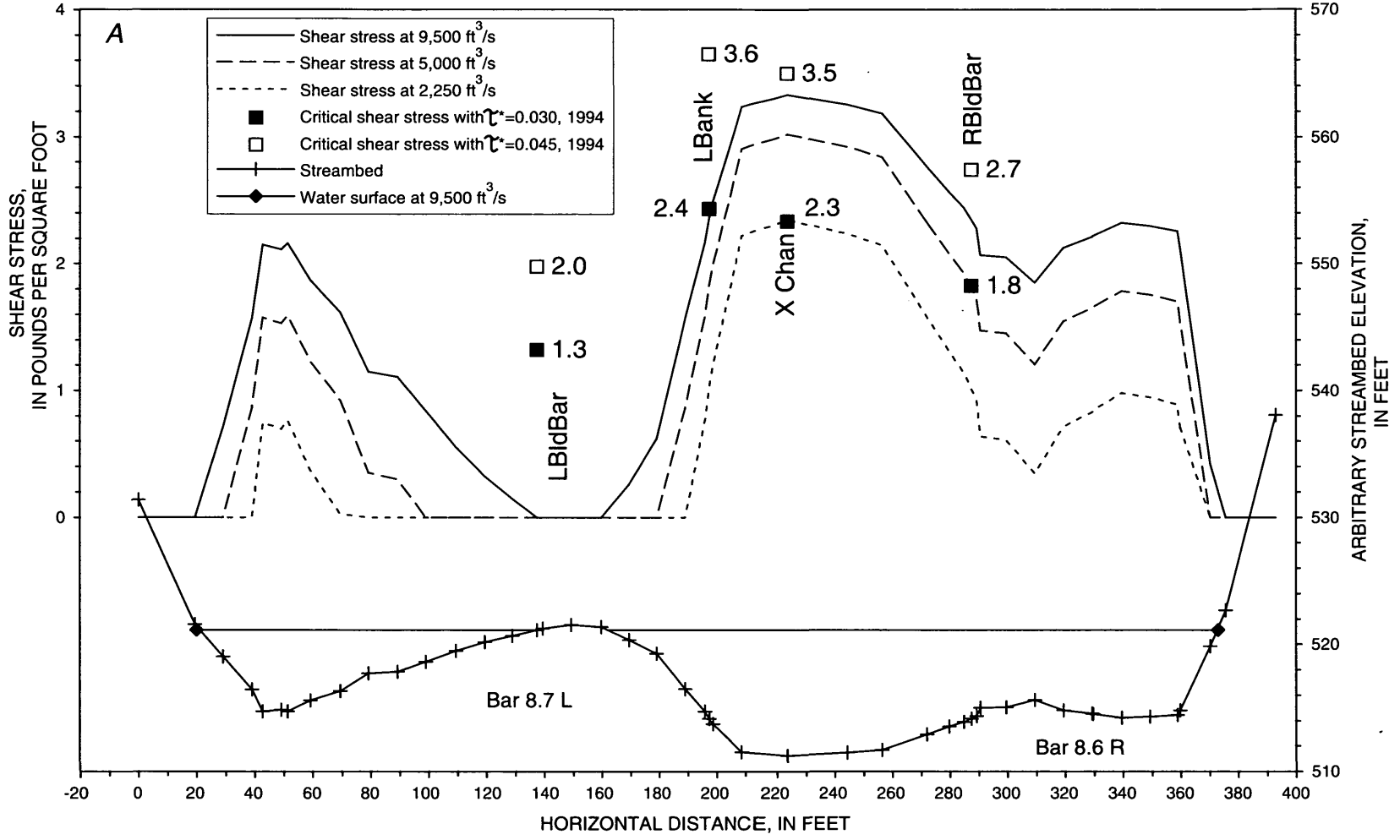

Figure 6. Plots showing channel cross section, shear-stress distribution, and critical shear stress for sediment median particle size in the Warner Point study reach: (*A*) cross section V1, (*B*) cross section V2, (*C*) cross section H60, (*D*) cross section H3, (*E*) cross section V3, (*F*) cross section V4, (*G*) cross section V5, and (*H*) cross section H9 (study reach shown in fig. 4).

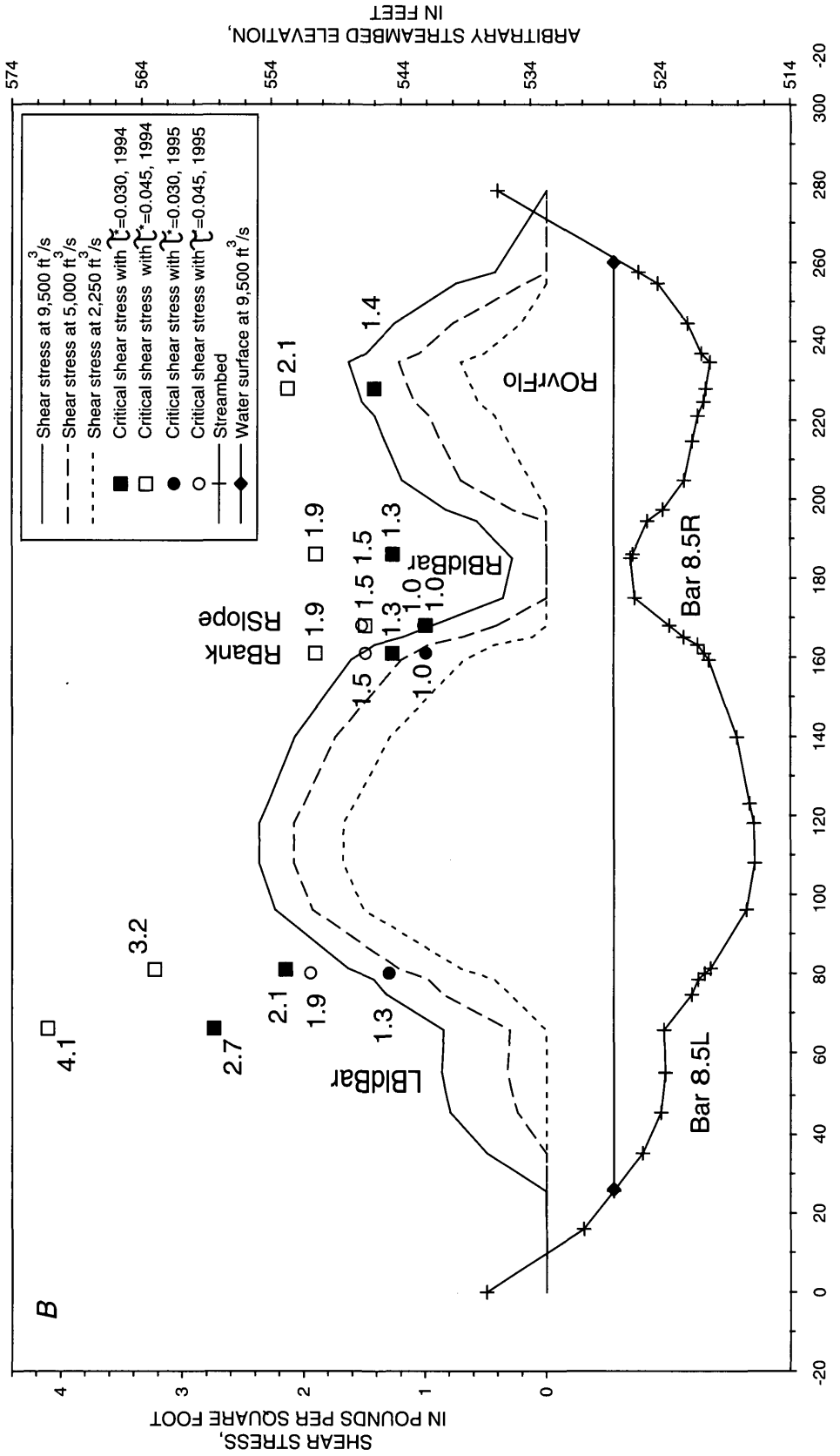

Figure 6. Plots showing channel cross section, shear-stress distribution, and critical shear stress for sediment median particle size in the Warner Point study reach: (*A*) cross section V1, (*B*) cross section V2, (*C*) cross section H60, (*D*) cross section H3, (*E*) cross section V3, (*F*) cross section V4, (*G*) cross section V5, and (H) cross section H9 (study reach shown in fig. 4)—Continued.

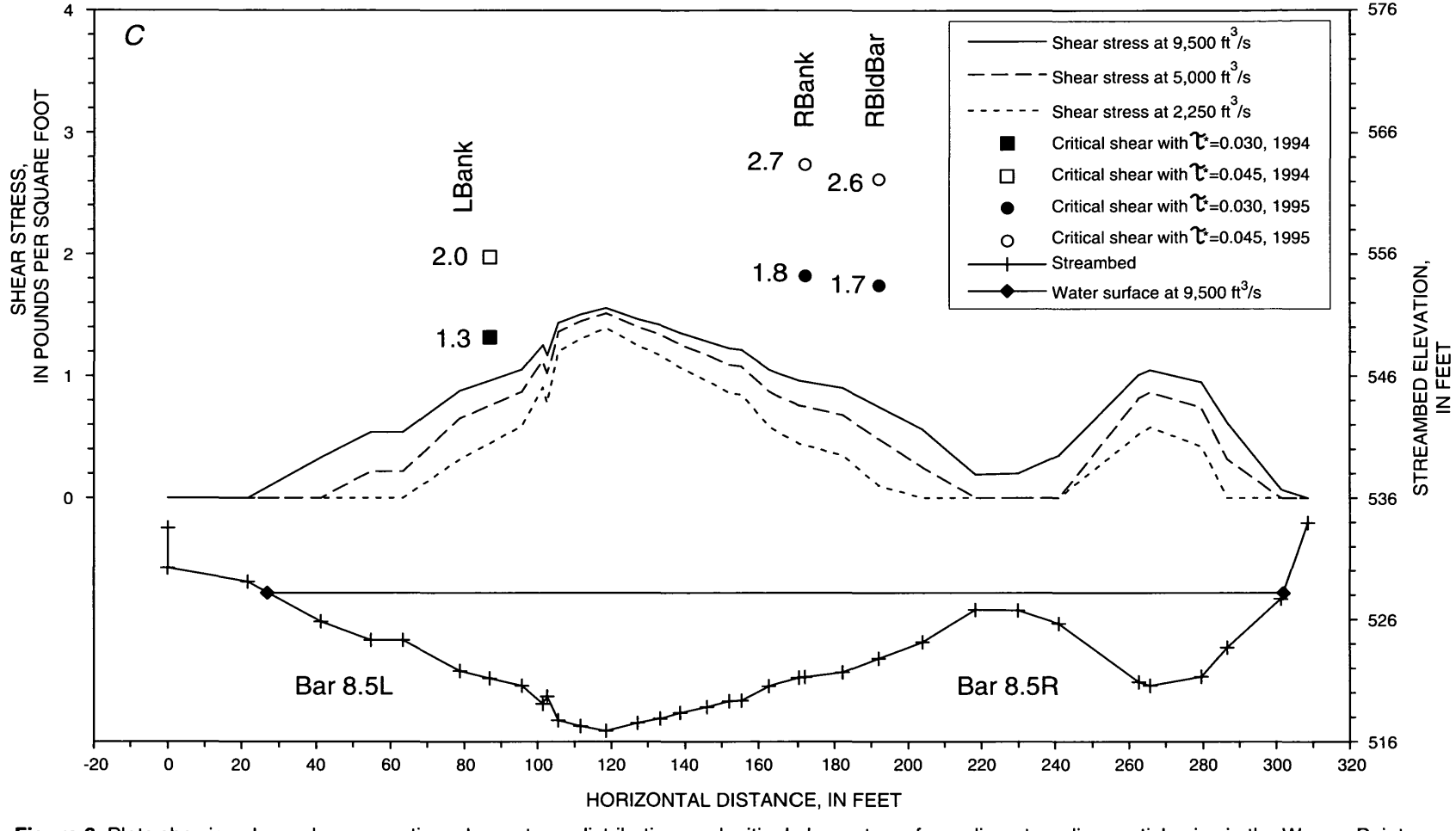

Figure 6. Plots showing channel cross section, shear-stress distribution, and critical shear stress for sediment median particle size in the Warner Point study reach: (*A*) cross section V1, (*B*) cross section V2, (*C*) cross section H60, (*D*) cross section H3, (*E*) cross section V3, (*F*) cross section V4, (*G*) cross section V5, and (*H*) cross section H9 (study reach shown in fig. 4)—Continued.

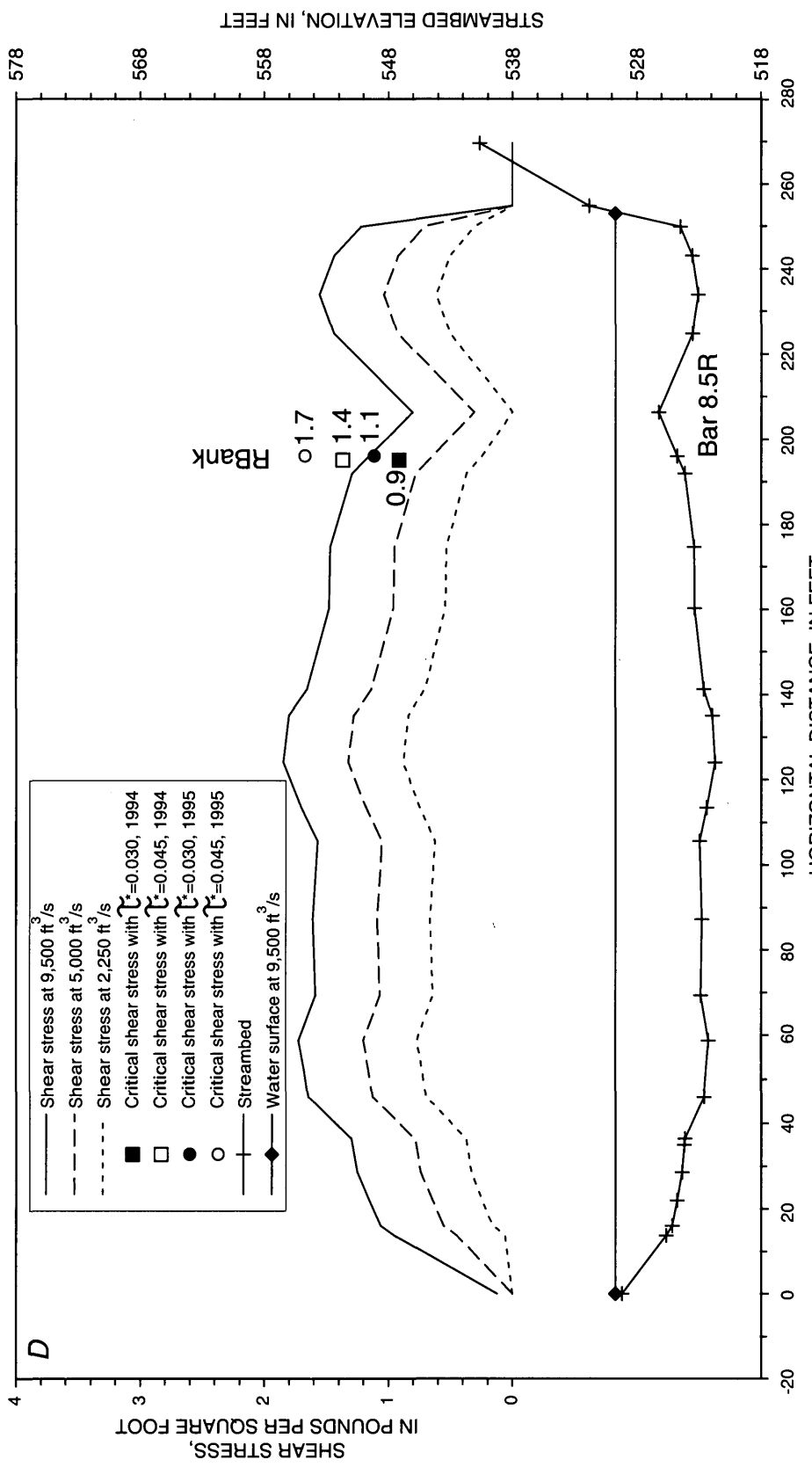

Figure 6. Plots showing channel cross section, shear-stress distribution, and critical shear stress for sediment median particle size in the Warner Point study reach: (*A*) cross section V1, (*B*) cross section V2, (*C*) cross section H60, (*D*) cross section H3, (*E*) cross section V3, (*F*) cross section V4, (*G*) cross section V5, and (*H*) cross section H9 (study reach shown in fig. 4)—Continued.

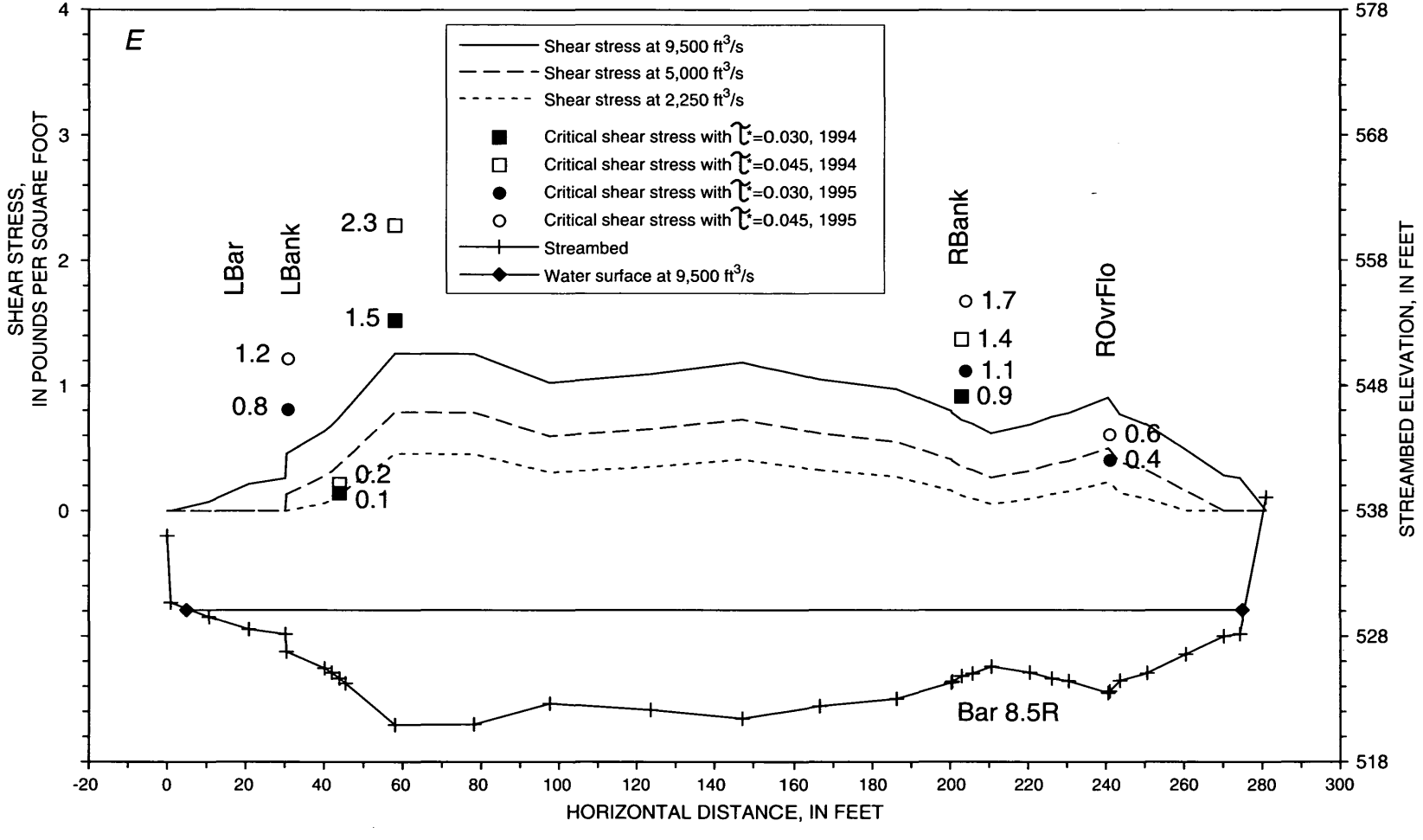

Figure 6. Plots showing channel cross section, shear-stress distribution, and critical shear stress for sediment median particle size in the Warner Point study reach: (*A*) cross section V1, (*B*) cross section V2, (*C*) cross section H60, (*D*) cross section H3, (*E*) cross section V3, (*F*) cross section V4, (*G*) cross section V5, and (*H*) cross section H9 (study reach shown in fig. 4)—Continued.

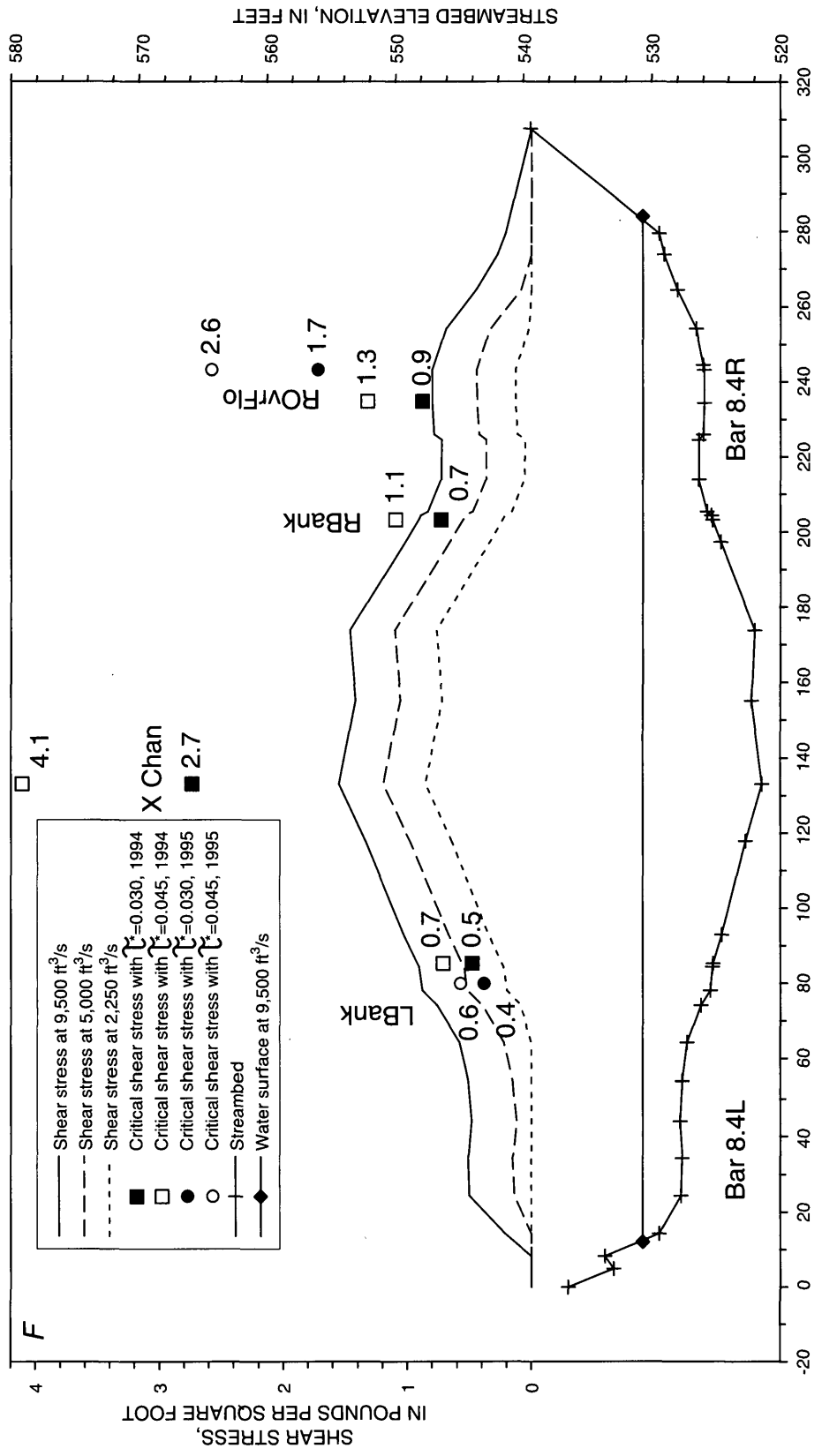

Figure 6. Plots showing channel cross section, shear-stress distribution, and critical shear stress for sediment median particle size in the Warner Point study reach: (*A*) cross section V1, (*B*) cross section V2, (*C*) cross section H60, (*D*) cross section H3, (*E*) cross section V3, (*F*) cross section V4, (*G*) cross section V5, and (*H*) cross section H9 (study reach shown in fig. 4)—Continued.

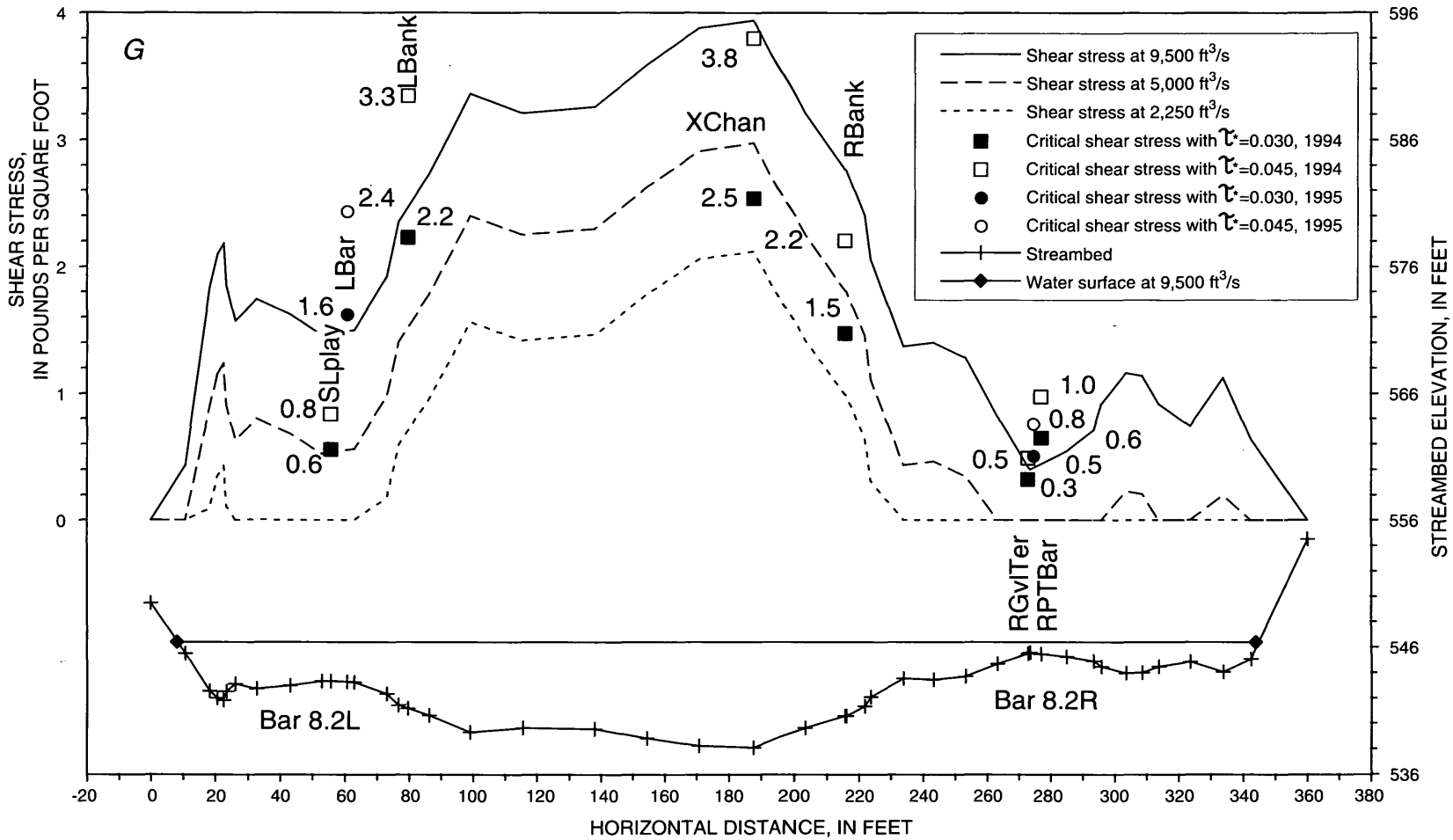

Figure 6. Plots showing channel cross section, shear-stress distribution, and critical shear stress for sediment median particle size in the Warner Point study reach: (*A*) cross section V1, (*B*) cross section V2, (*C*) cross section H60, (*D*) cross section H3, (*E*) cross section V3, (*F*) cross section V4, (*G*) cross section V5, and (*H*) cross section H9 (study reach shown in fig. 4)—Continued.

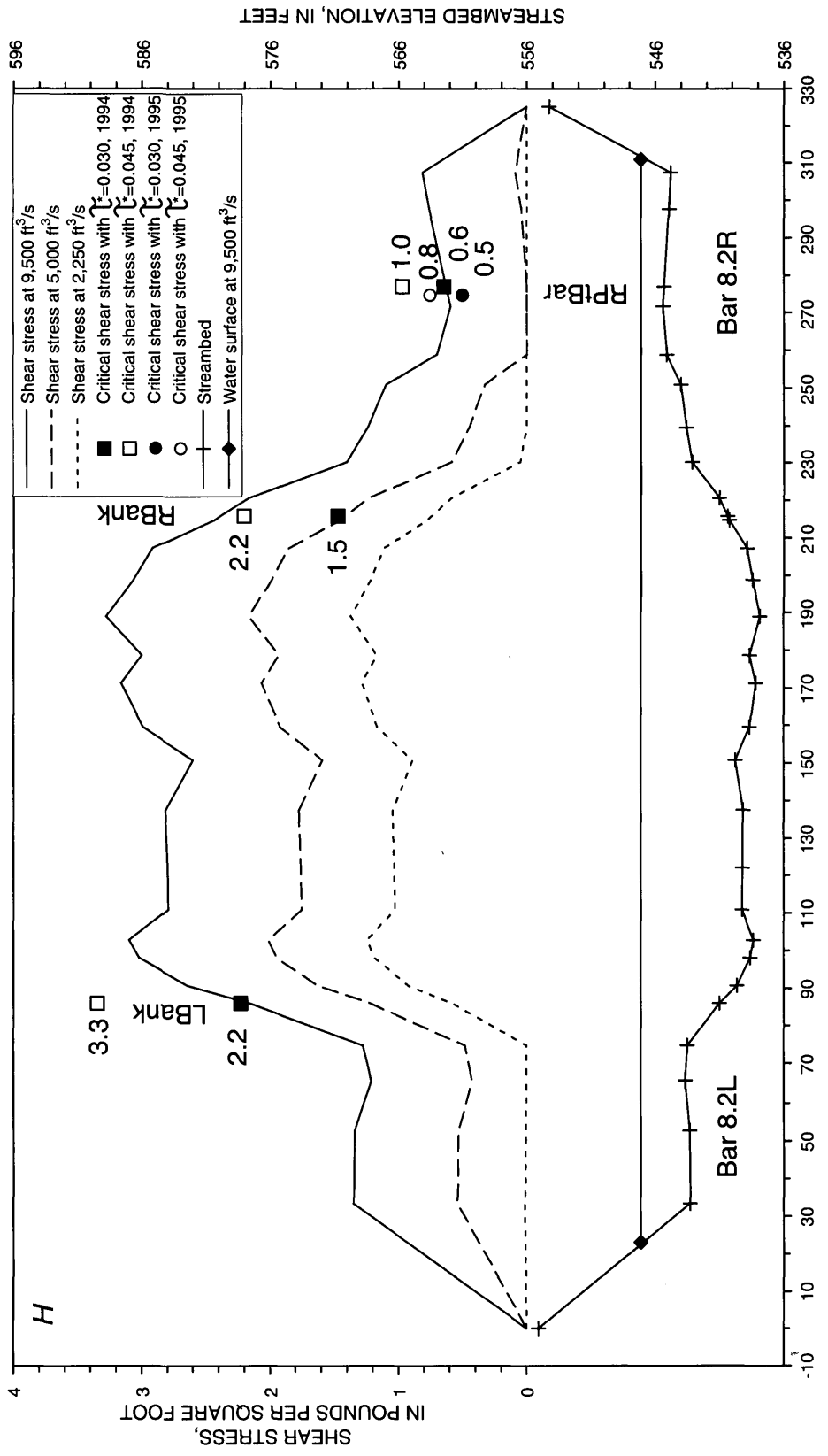

Figure 6. Plots showing channel cross section, shear-stress distribution, and critical shear stress for sediment median particle size in the Warner Point study reach: (*A*) cross section V1, (*B*) cross section V2, (*C*) cross section H60, (*D*) cross section H3, (*E*) cross section V3, (*F*) cross section V4, (*G*) cross section V5, and (*H*) cross section H9 (study reach shown in fig. 4)—Continued.

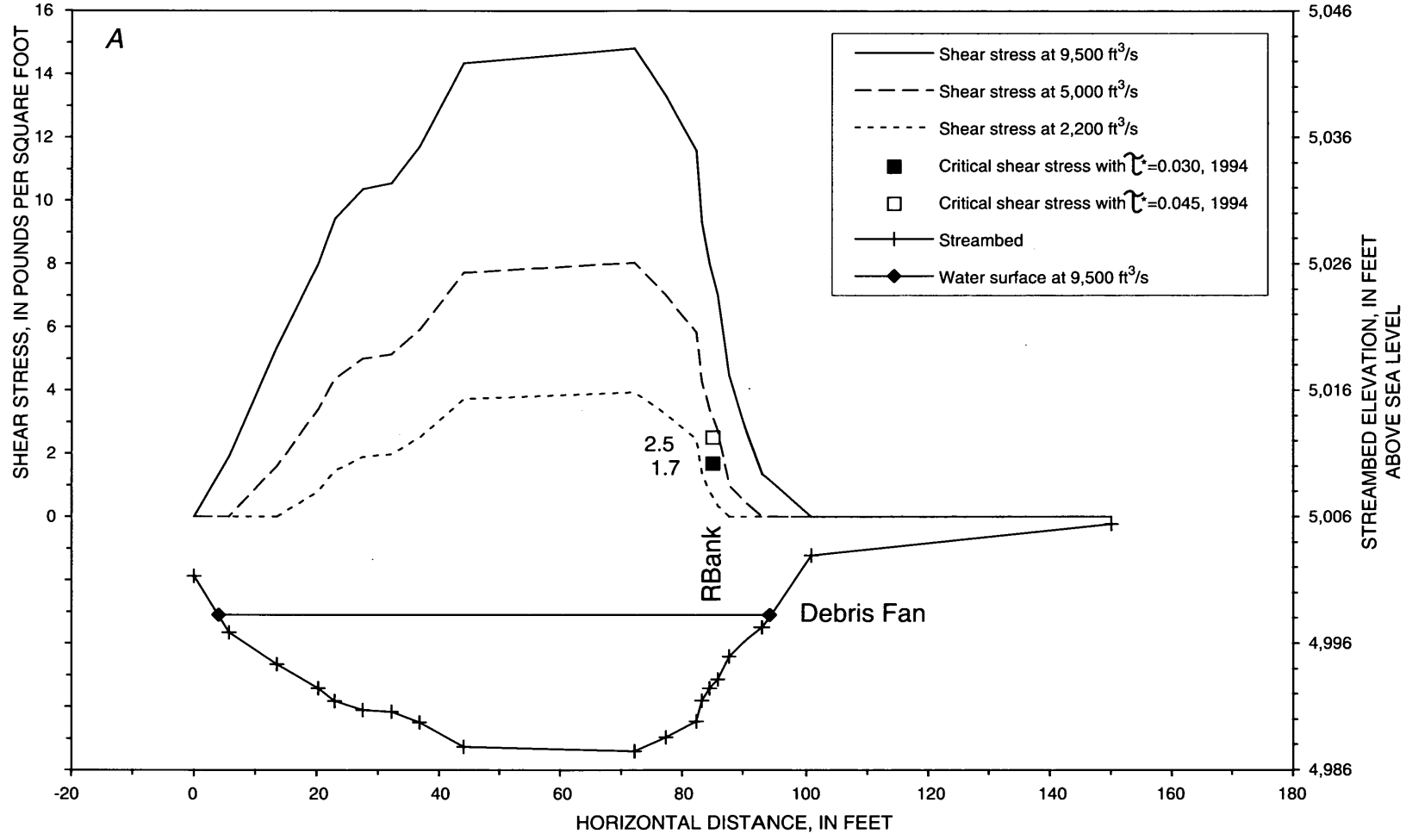

Figure 7. Plots showing channel cross section, shear-stress distribution, and critical shear stress for sediment median particle size in the Red Rock Canyon study reach, (*A*) cross section F2, (*B*) cross section F1, (*C*) cross section H1, (*D*) cross section H2, (*E*) cross section G1, and (*F*) cross section G2. (study reach shown in fig. 5).

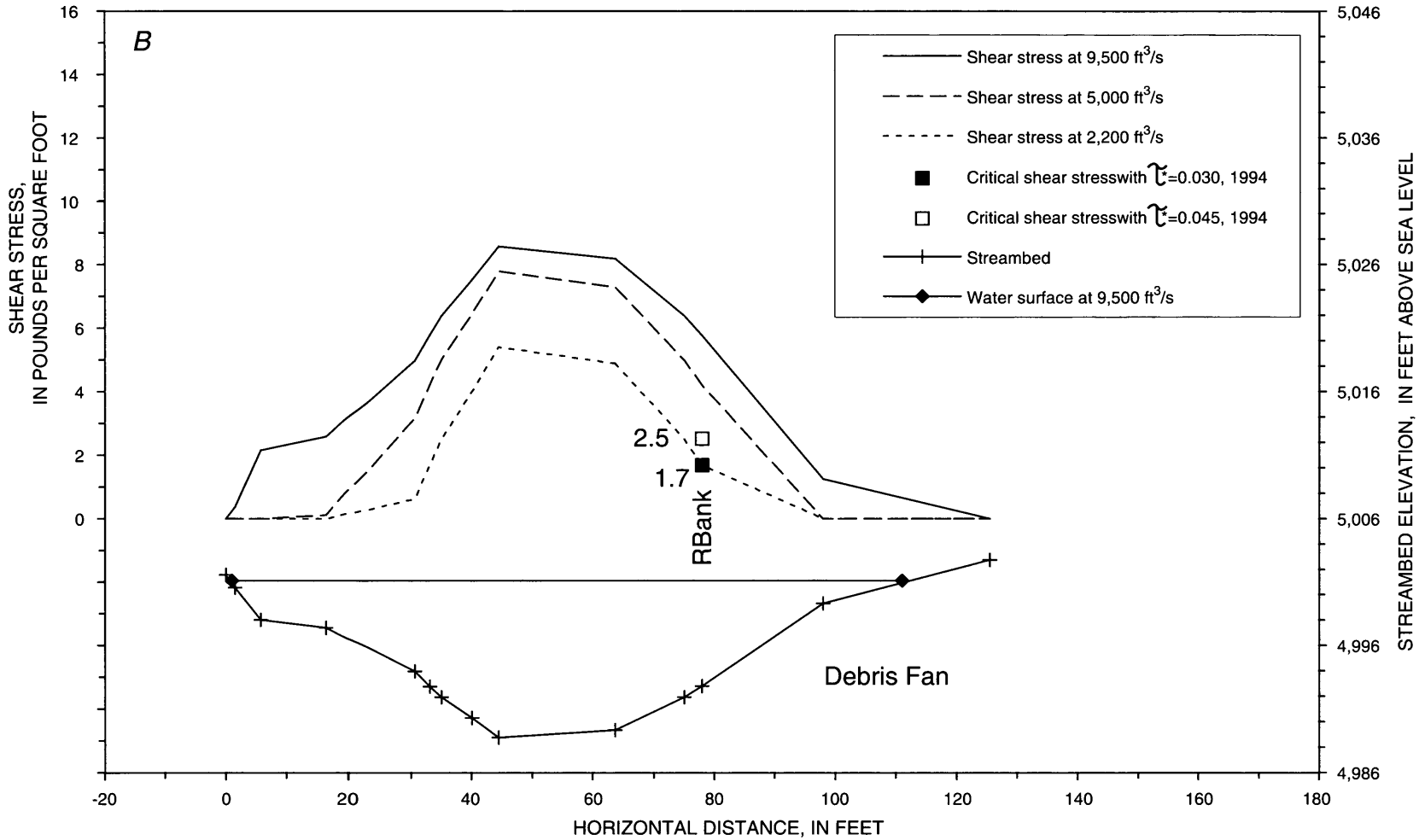

Figure 7. Plots showing channel cross section, shear-stress distribution, and critical shear stress for sediment median particle size in the Red Rock Canyon study reach, (*A*) cross section F2, (*B*) cross section F1, (*C*) cross section H1, (*D*) cross section H2, (*E*) cross section G1, and (*F*) cross section G2. (study reach shown in fig. 5)—Continued.

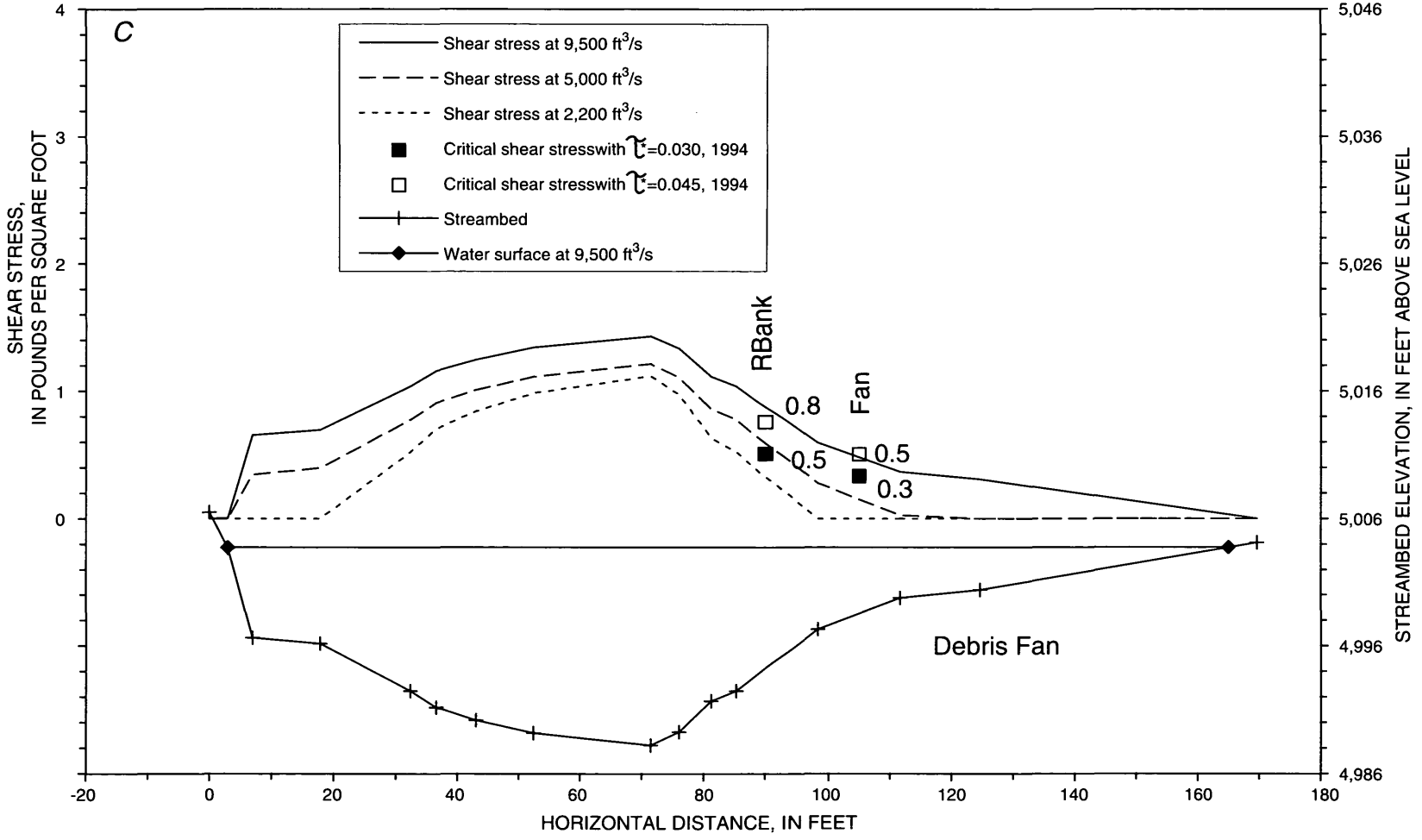

Figure 7. Plots showing channel cross section, shear-stress distribution, and critical shear stress for sediment median particle size in the Red Rock Canyon study reach, (*A*) cross section F2, (*B*) cross section F1, (*C*) cross section H1, (*D*) cross section H2, (*E*) cross section G1, and (*F*) cross section G2. (study reach shown in fig. 5)—Continued.

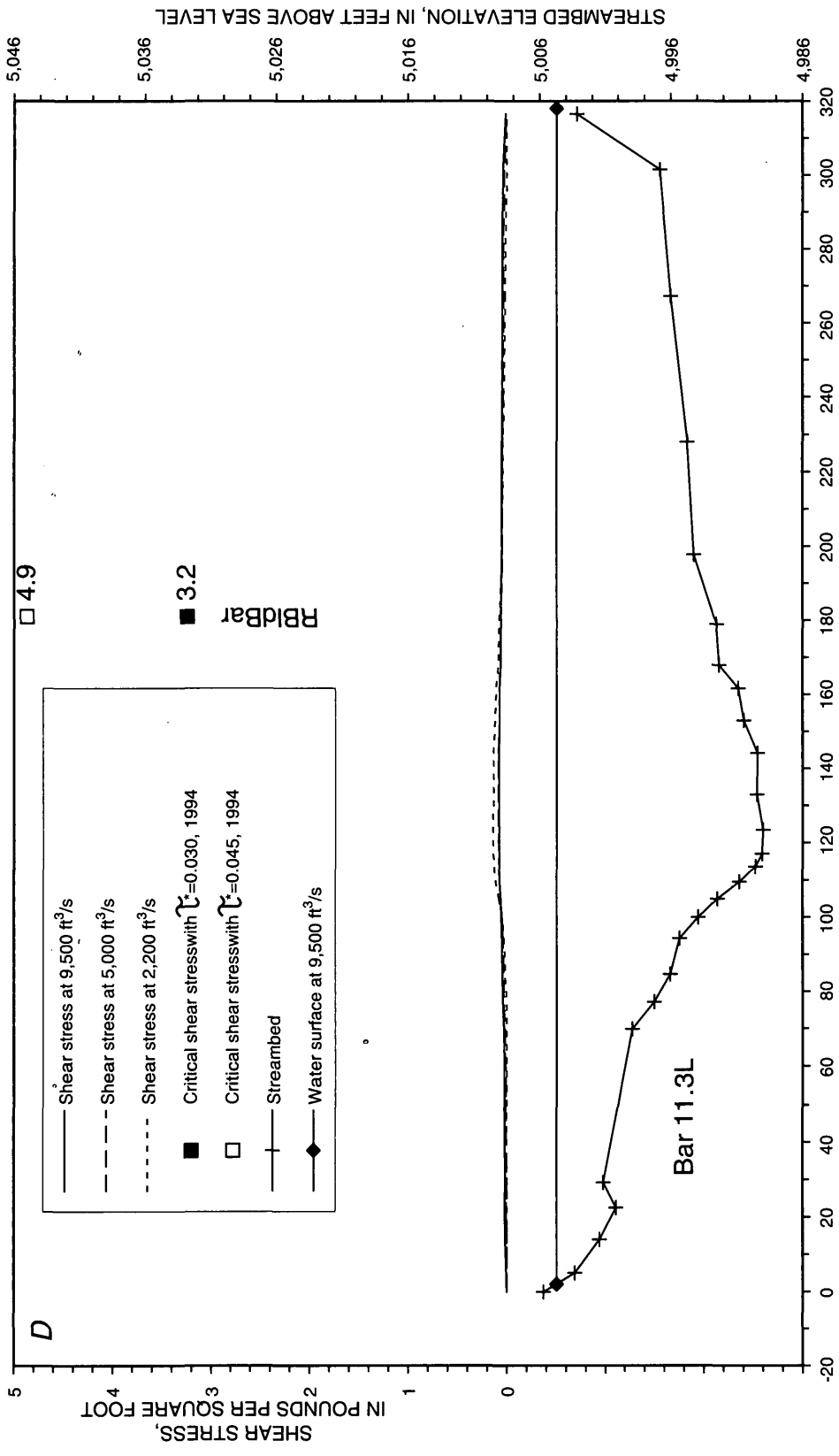

Figure 7. Plots showing channel cross section, shear-stress distribution, and critical shear stress for sediment median particle size in the Red Rock Canyon study reach, (*A*) cross section F2, (*B*) cross section F1, (*C*) cross section H1, (*D*) cross section H2, (*E*) cross section G1, and (*F*) cross section G2. (study reach shown in fig. 5)—Continued.

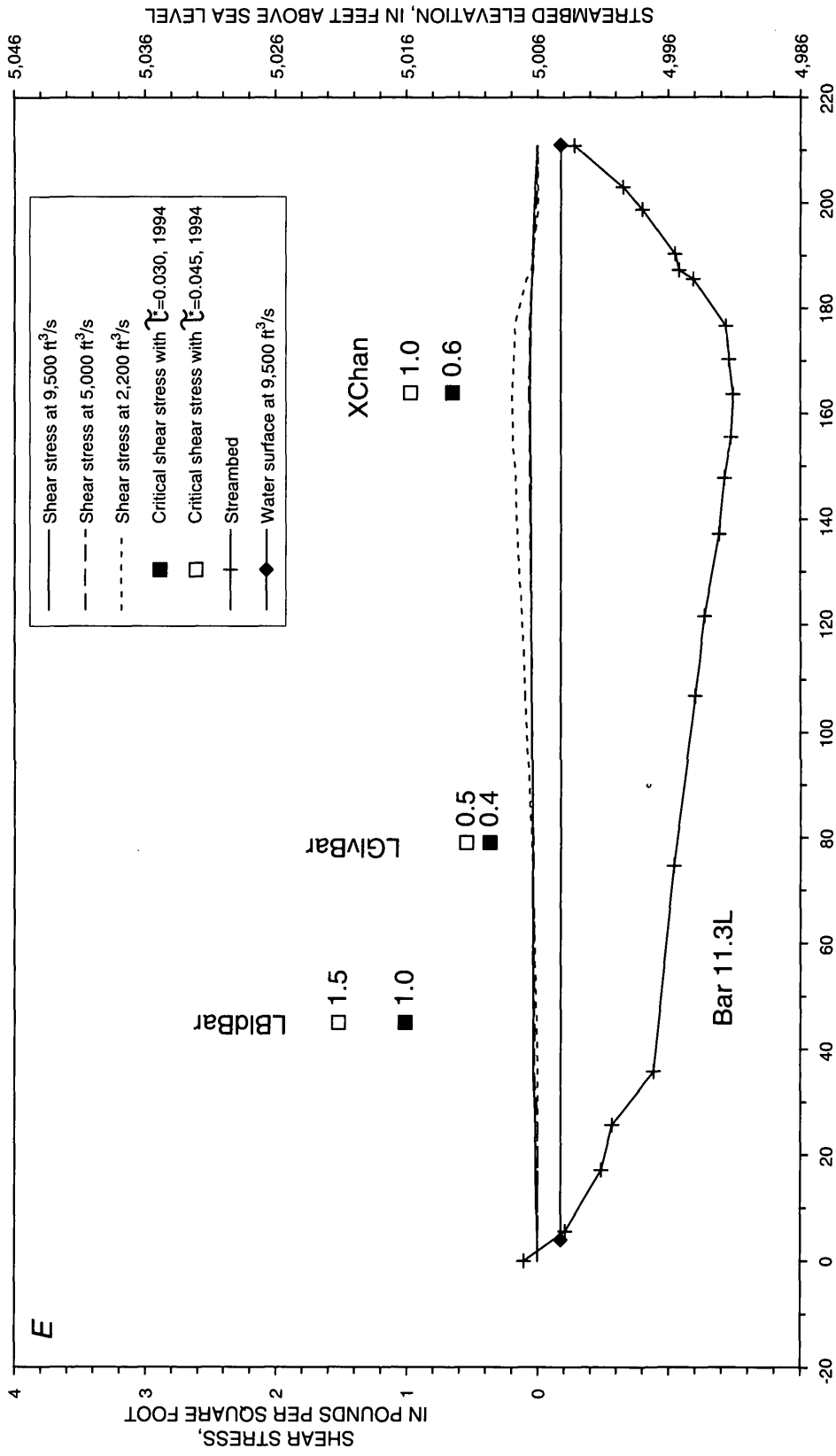

Figure 7. Plots showing channel cross section, shear-stress distribution, and critical shear stress for sediment median particle size in the Red Rock Canyon study reach, (*A*) cross section F2, (*B*) cross section F1, (*C*) cross section H1, (*D*) cross section H2, (*E*) cross section G1, and (*F*) cross section G2. (study reach shown in fig. 5)—Continued.

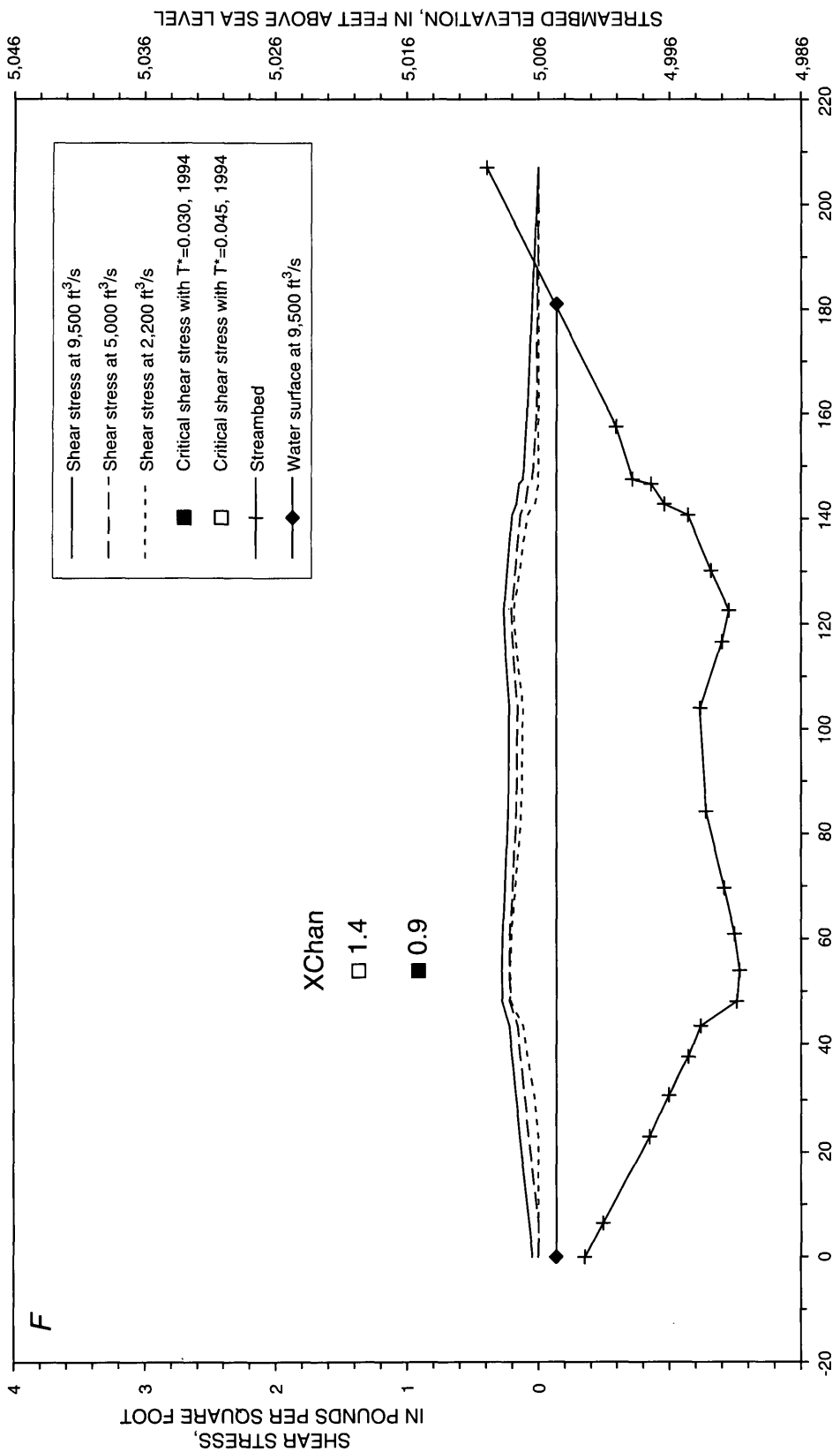

Figure 7. Plots showing channel cross section, shear-stress distribution, and critical shear stress for sediment median particle size in the Red Rock Canyon study reach, (*A*) cross section F2, (*B*) cross section F1, (*C*) cross section H1, (*D*) cross section H2, (*E*) cross section G1, and (*F*) cross section G2. (*study reach shown in fig. 5*)—Continued.

with sheltered particles, interlocked grains, or strong imbrication) had τ^*_c between 0.055 and 0.067, whereas loosely structured beds (those with an open-particle framework) had τ^*_c between 0.0096 and 0.011.

The BLCA investigation did not include onsite observations of sediment entrainment and measurement of actual hydraulic conditions at the moment of sediment entrainment; therefore, the Shields parameter could not be precisely determined in this study as in some flume and instrumented field studies. Critical shear stresses for each sediment measurement were calculated with Shields τ^*_c values of 0.030 and 0.045 to provide a range of the most likely entraining conditions (tables 3 and 4). Figures 6 and 7 show the lateral locations of sediment particle-size measurements and corresponding estimates of the critical shear stress for entrainment of sediment d_{50} from the streambanks, alluvial bars, and overflow channels. Critical shear stress estimates for entrainment of sediment d_{50} from the streambed (XChan in tables 3 and 4) are shown at the lateral location of the thalweg, or the deepest point of the channel cross section, in figures 6 and 7.

Reworked bank and bar sediments were observed at several measurement sites following the 1995 peak discharge (9,470 ft^3/s). Using reconstructed flow depths and shear stresses associated with the peak discharge (Elliott and Hammack, in press), it appears that a Shields τ^*_c value of 0.030 rather than 0.045 may provide the better estimates of critical shear stresses, τ_c, and sediment entrainment at some locations in BLCA. Evidence of sediment entrainment or absence of sediment entrainment on inundated sediment-measurement sites in the Warner Point study reach after the 1995 peak discharge generally was consistent with critical shear stresses estimated using τ^*_c of 0.030 and with the boundary shear stress generated by the discharge peak (figs. 6*B*–6*H*).

Sediment was entrained by the 1995 peak discharge at all sediment-measurement sites on the distal margin of the debris fan in the Red Rock Canyon study reach. However, a recommended value of τ^*_c could not be empirically determined because 1995 flood shear stresses were sufficiently larger than τ_c calculated with τ^*_c values of either 0.030 or 0.045 (figs. 7*A*–7*C*). Entrainment of sediment d_{50} probably occurred at a discharge much less than the 1995 peak discharge; therefore, threshold conditions could not be reconstructed using high-water marks as at other BLCA cross sections.

Onsite examination of a low-elevation gravel bar at cross section G1 in the Red Rock Canyon reach (see figs. 14*A* and 14*B* in appendix at back of report) indicated that sediment entrainment and reworking had occurred during the 1995 discharge peak. The relatively small d_{50} (36 mm, table 4) of this deposit and its proximity to the left low-flow bank implied that τ_c probably was exceeded by a discharge much less than the 1995 flood peak. The boundary shear stresses, τ_o, calculated for the three reference discharges using HEC-RAS output clearly were much lower than the actual shear stresses at this location (fig. 7*E*). A likely explanation for the underestimated τ_o is based on the limitations of a one-dimensional, water-surface profiles model when applied to a reach upstream from a significant lateral constriction such as the debris fan at the mouth of Tributary 11.3R in the Red Rock Canyon study reach (fig. 5). When discharge exceeds 2,200 to 3,000 ft^3/s, a large, recirculating eddy develops on the right bank upstream from the debris fan, resulting in higher than anticipated velocities and shear stresses on the inundated left bank. The clear discrepancy between predicted τ_o and observed sediment reworking at cross section G1 illustrates a situation in which the one-dimensional model was inappropriately applied. Consequently, HEC-RAS-derived boundary shear-stress conditions upstream from the debris-fan constriction were not used in subsequent calculations or analyses (cross sections H2, G1, G2, G3, H3, and G4).

Sediment-entrainment potential for a variety of geomorphic surfaces can be expressed as the ratio of flood shear stress to the critical shear stress (τ_o/τ_c) for a range of discharges. The τ_o/τ_c ratio facilitates site-to-site comparison of the anticipated effects of specific discharges and integrates several geomorphic and sediment variables (flow depth, energy gradient, median particle size, critical shear stress) over a wide range of values (Elliott and Hammack, in press). Graphs of the sediment-entrainment potential for several selected geomorphic surfaces in the Warner Point (fig. 8) and Red Rock Canyon (fig. 9) study reaches provide a way to estimate the relative effects of different hypothetical peak discharges. The geomorphic surfaces examined included (a) low-flow banks (fig. 8*A*), surfaces subaerially exposed much of the year but inundated by discharges of approximately 700 to 900 ft^3/s (RI less than 1 year); (b) low-bar surfaces (fig. 8*B*), fluvial deposits inundated by approximately 2,000 to 4,000 ft^3/s (RI 1.2 to

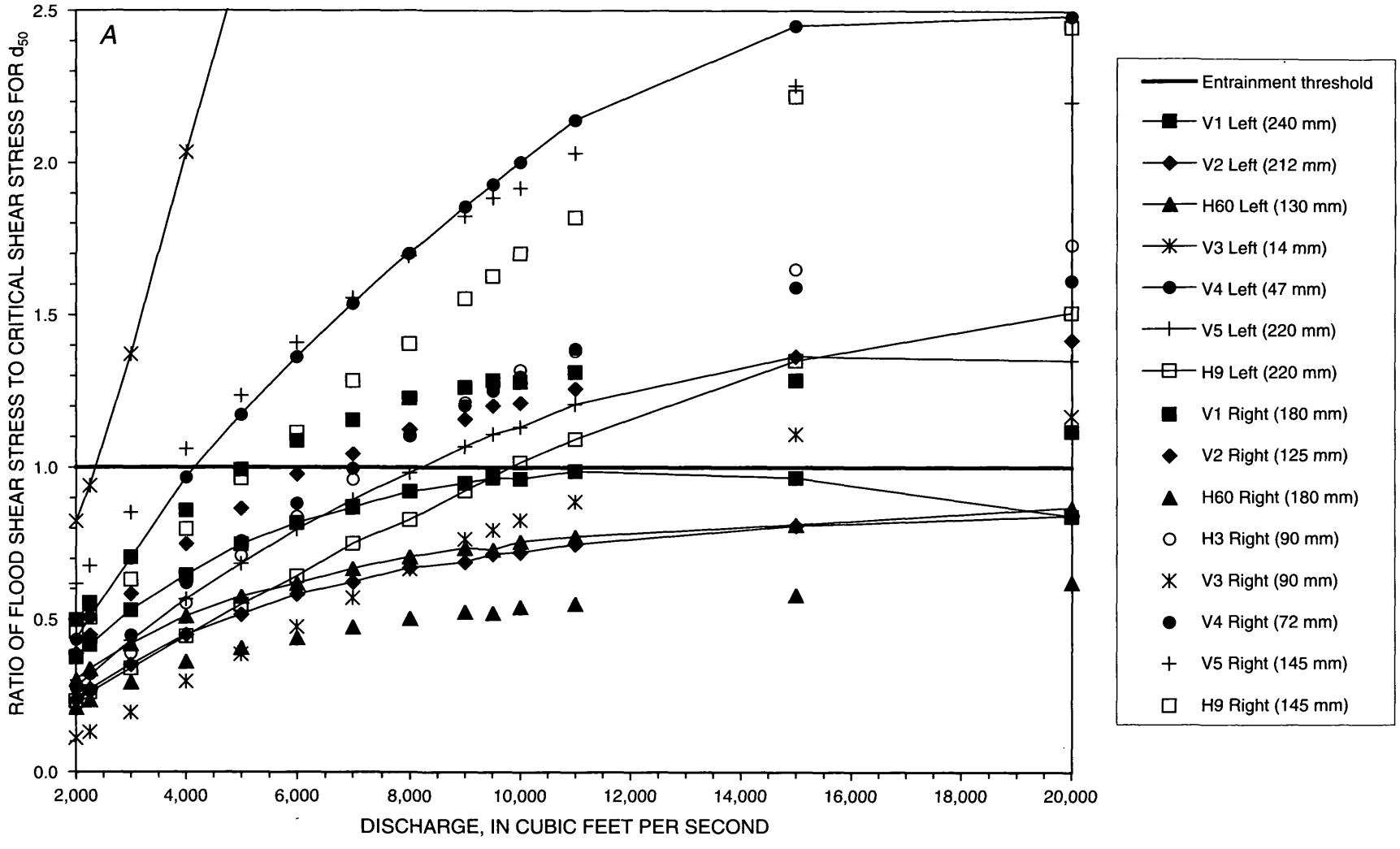

Figure 8. Plots showing sediment-entrainment potential on similar geomorphic surfaces in the Warner Point study reach: (*A*) low-flow banks, (*B*) low-bar surfaces, (*C*) high-bar surfaces, and (*D*) overflow channels. Median particle size of the surface is shown in parentheses.

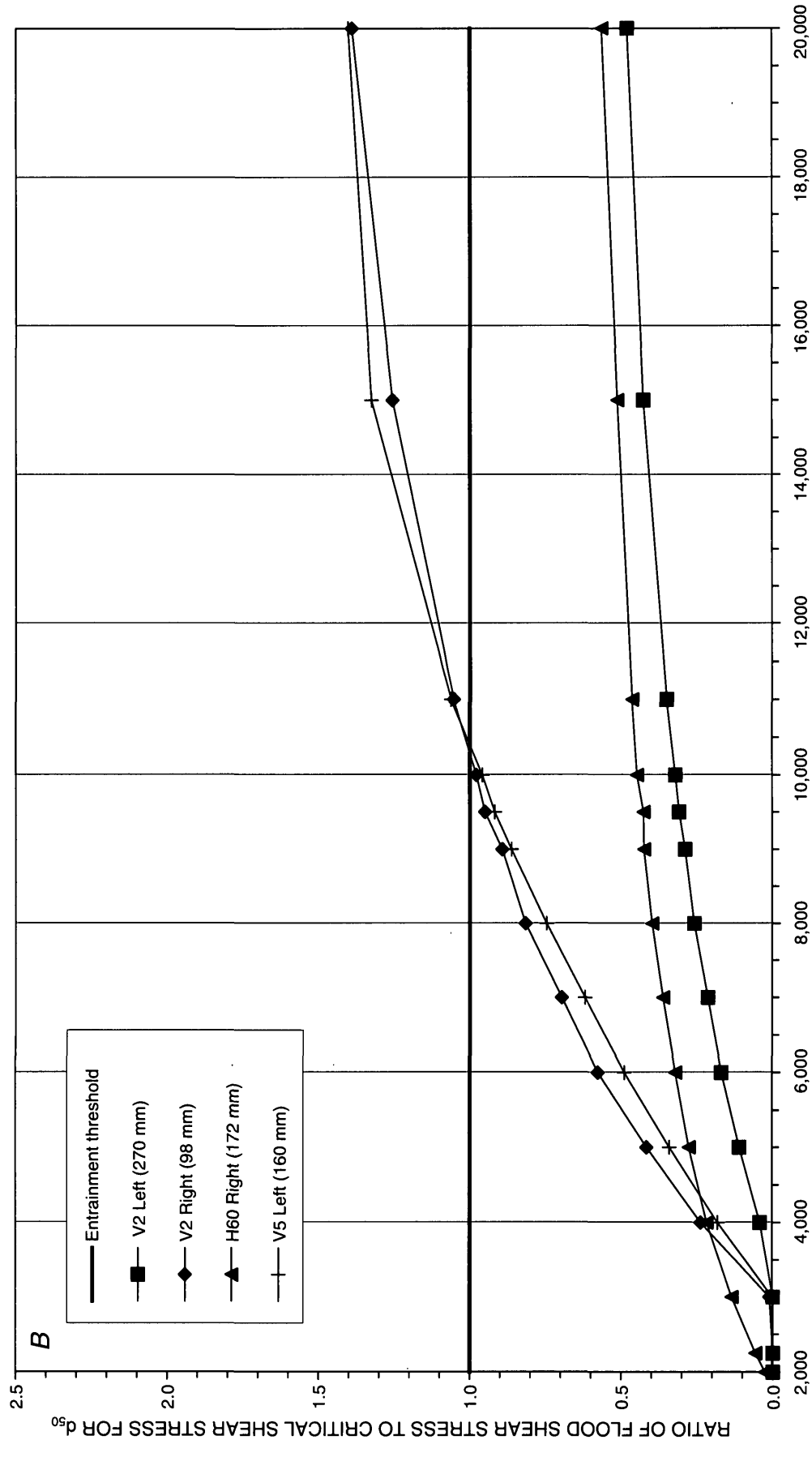

Figure 8. Plots showing sediment-entrainment potential on similar geomorphic surfaces in the Warner Point study reach: (*A*) low-flow banks, (*B*) low-bar surfaces, (*C*) high-bar surfaces, and (*D*) overflow channels. Median particle size of the surface is shown in parentheses—Continued.

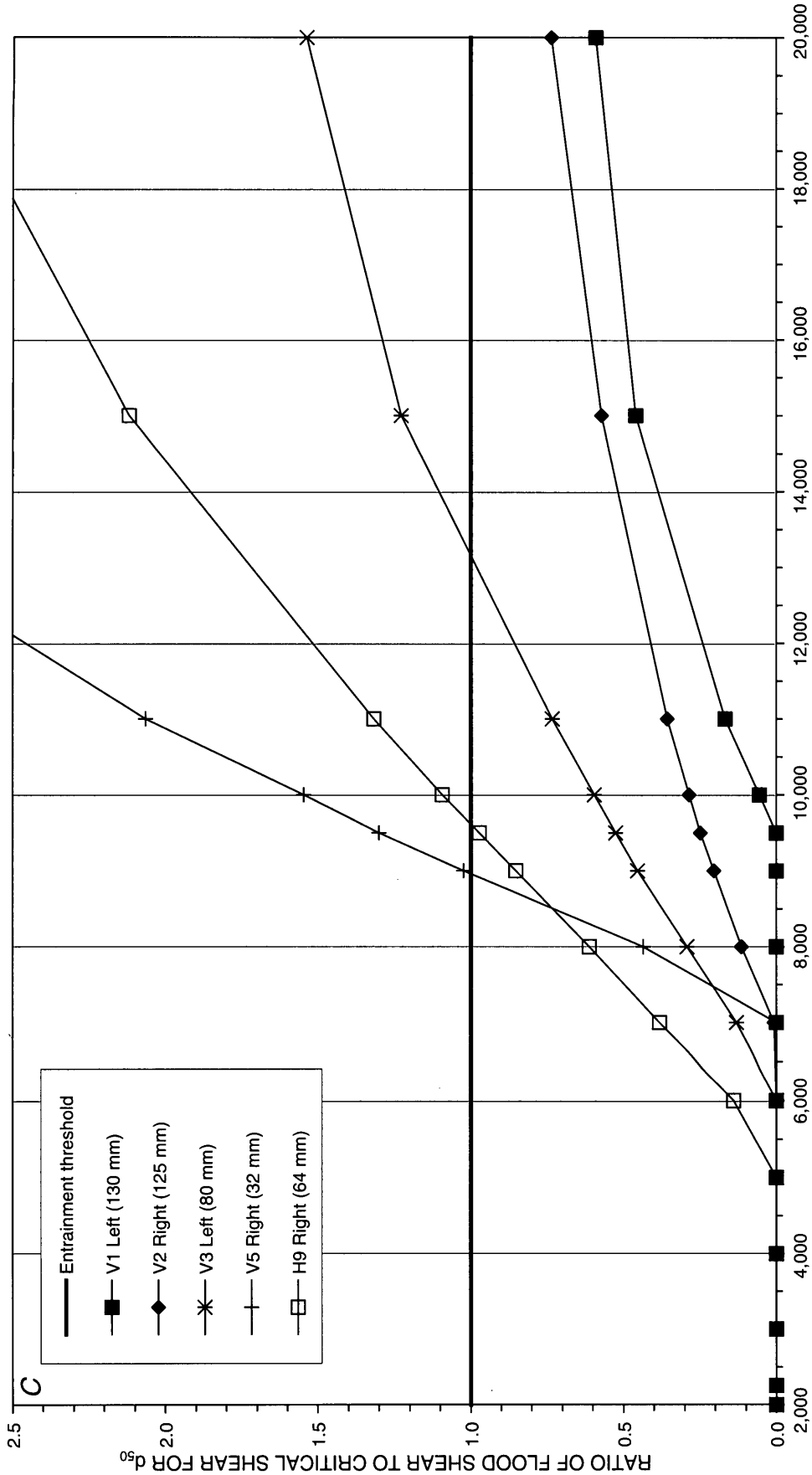

Figure 8. Plots showing sediment-entrainment potential on similar geomorphic surfaces in the Warner Point study reach: (*A*) low-flow banks, (*B*) low-bar surfaces, (*C*) high-bar surfaces, and (*D*) overflow channels. Median particle size of the surface is shown in parentheses—Continued.

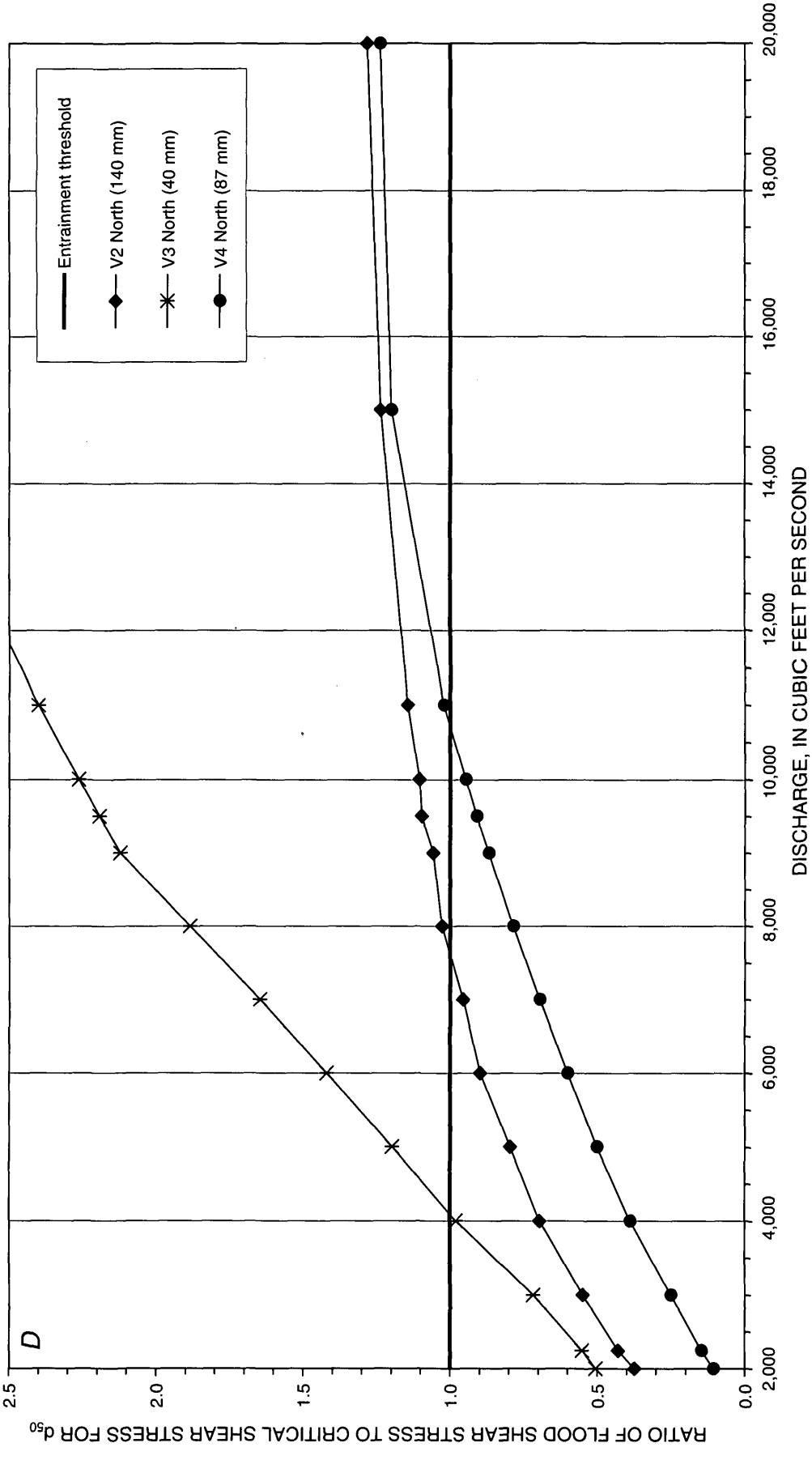

Figure 8. Plots showing sediment-entrainment potential on similar geomorphic surfaces in the Warner Point study reach: (*A*) low-flow banks, (*B*) low-bar surfaces, (*C*) high-bar surfaces, and (*D*) overflow channels. Median particle size of the surface is shown in parentheses—Continued.

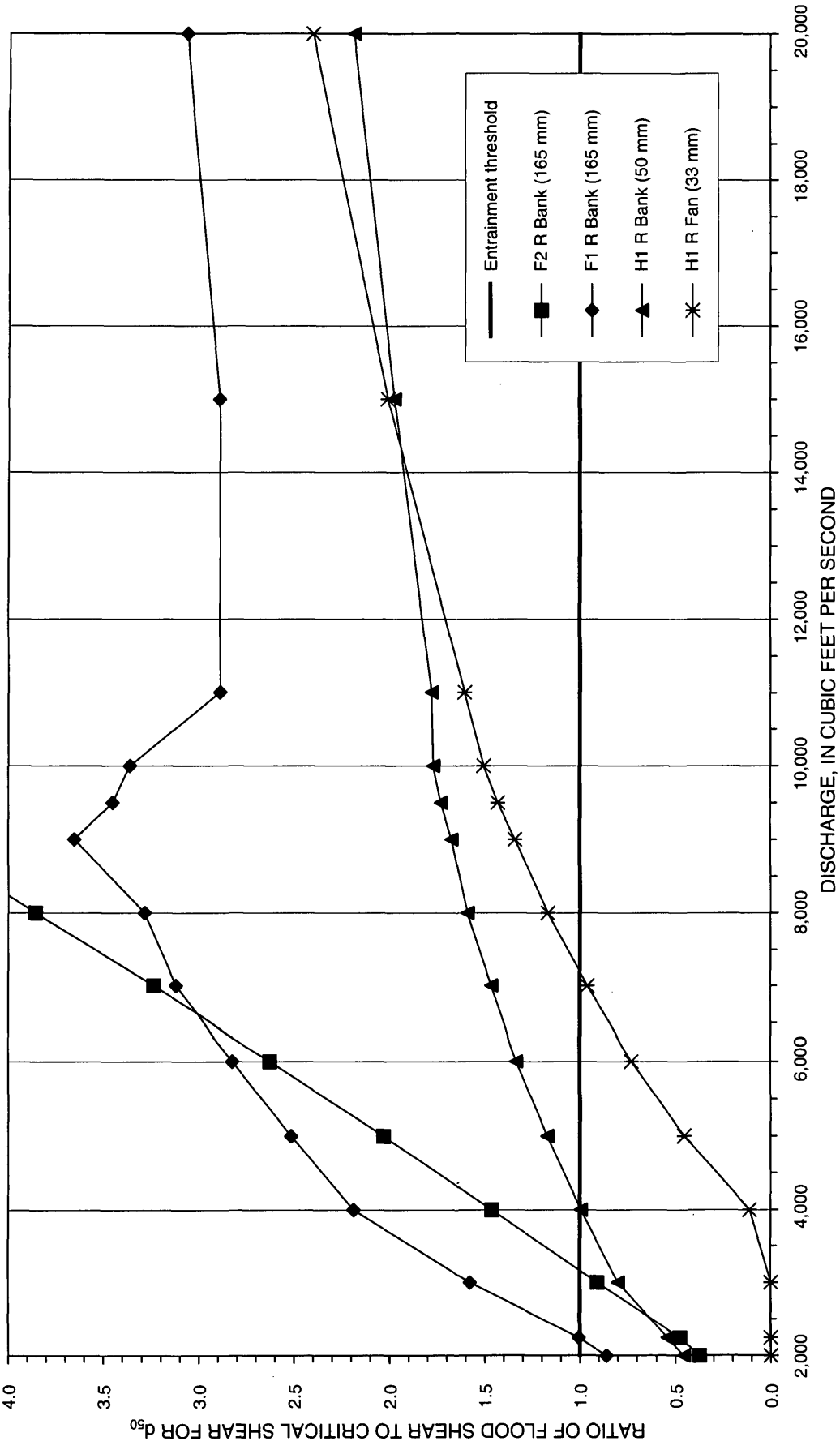

Figure 9. Plot showing sediment-entrainment potential on distal debris-fan surfaces in the Red Rock Canyon study reach. Median particle size of the surface is shown in parentheses.

2.5 years); (c) high-bar surfaces (fig. 8*C*), fluvial deposits inundated by approximately 6,000 to 10,000 ft^3/s (RI 6 to 35 years); (d) overflow channels (fig. 8*D*), water courses situated between large fluvial bars and adjacent talus slopes inundated by approximately 500 to 1,500 ft^3/s (RI less than 1 year); and (e) a recent tributary debris-flow deposit (fig. 9) inundated by approximately 4,000 ft^3/s (RI 2.5 years).

A τ^*_c value of 0.030 and the sediment d_{50} were used in the calculations represented in figures 8 and 9. In most locations, τ_o increases with discharge, whereas τ_c is constant for a given sediment d_{50}. The ratio of τ_o/τ_c generally increases with discharge, although the rate of change and the value of τ_o/τ_c vary with channel configuration, local energy gradient, and sediment size. Entrainment is anticipated, and the critical discharge is attained when τ_o/τ_c exceeds a threshold value of 1.0; but as figures 8 and 9 illustrate, the critical discharge is not unique for similar geomorphic surfaces at different cross sections. Differing entrainment potential for similar geomorphic surfaces (low-flow banks, low-elevation bars, high-elevation bars, and so forth) indicates that estimation of minimum streamflow requirements based on sediment mobility requires site-specific geomorphic and sedimentologic data.

The left banks at cross sections V1, V2, and H60 (fig. 8*A*), the right bank at H60 (fig. 8*A*), the left low bar at cross section V2 (fig. 8*B*), and the right low bar at cross section H60 (fig. 8*B*, shown in figs. 13*A* and 13*B* in appendix) are relatively coarse and potentially are exposed to very high shear stresses. However, the τ_o/τ_c curves for these sites appear to be asymptotic with respect to the entrainment threshold line, indicating that entrainment of d_{50} from these surfaces is unlikely at any discharge. One possible explanation is that the sediment of Bars 8.7L, 8.5L, and 8.5R (fig. 4) may be vestiges of an earlier, more competent flow regime or of different channel configurations such that no discharge, at least as large as the modeled 20,000 ft^3/s, will entrain d_{50}, given the present channel geometry.

SUMMARY

The Black Canyon of the Gunnison River in western Colorado, known for its precipitous bedrock exposures and gorge-like characteristics, also includes several alluvial reaches that are potentially sensitive to changes in streamflow. Sediment, derived from talus slopes, rockfall, and tributary debris flows, periodically is reworked and redeposited on the streambed, streambanks, and alternate bars in these alluvial reaches. Geomorphic and sedimentologic data were collected from two alluvial reaches in the Black Canyon of the Gunnison National Monument (BLCA)—the Warner Point study reach and the Red Rock Canyon study reach. These data and hydrologic records from an upstream gaging station were used to calculate the entrainment potential of a large size-range of sediment on a variety of fluvial geomorphic surfaces typical of the Black Canyon and other canyon rivers.

The Gunnison River hydrology is dominated by snowmelt runoff; however, impoundments and diversion upstream from BLCA have affected the streamflow magnitude and duration since 1966. The 10-year flood decreased from 14,900 to 7,000 ft^3/s and the 5-year flood from 12,700 to 5,460 ft^3/s. While reservoir operation has attenuated flood peaks in BLCA, it also has augmented moderate streamflows. The duration of streamflows between 1,140 and 3,000 ft^3/s has increased from an average of 12 percent of the time, an average of about 44 days per year (1911–65), to 38 percent of the time, an average of about 139 days per year (1966–94).

The one-dimensional water-surface profiles models HEC-2 and HEC-RAS were used to estimate water-surface elevations, flow depths, and hydraulic conditions through the study reaches for a range of discharges from 2,000 to 20,000 ft^3/s. These models used surveyed channel cross sections and were calibrated with observed water-surface elevations and high-water marks in the Warner Point and Red Rock Canyon reaches. The HEC-2 models were calibrated by varying the Manning's n roughness coefficient until the estimated water-surface elevations nearly equaled the surveyed water-surface elevations. Discharges at the Warner Point and Red Rock Canyon reaches were assumed to be comparable to discharges recorded a few hours earlier at USGS gaging station 09128000 upstream.

The hydraulic models appeared to adequately simulate observed water surfaces and hydraulic conditions except in the reach affected by backwater and a large, high-flow, recirculating eddy upstream from the debris-flow constriction in the Red Rock Canyon study reach. Estimated water-surface elevations were very close to surveyed elevations for most calibration

discharges having differences less than 10 percent of the calculated maximum flow depth for a specific discharge. HEC-2 and HEC-RAS output from the modeling runs included water-surface elevations and energy gradients, from which flow depths and boundary shear stresses at specific locations on the cross sections were calculated.

The low-flow channel of most cross sections in the study reaches is composed of material in the large cobble- and boulder-size range; however, streambanks and bars are composed of finer material in the gravel-, cobble-, and occasionally boulder-size range. Shear stresses acting on the streambed, on streambanks, and on inundated alluvial bars is highly variable for any specific discharge and is dependent, in part, on the local flow depth and energy gradient of the river. Consequently, conditions for sediment entrainment, sorting, and deposition also are spatially variable. Data from the hydraulic models and sediment data measured at several locations were used to calculate the entrainment potential of a wide range of sediment sizes on several geomorphic surfaces. Sediment entrainment is anticipated when the local boundary shear stress, τ_o, exceeds the critical shear stress, τ_c, of the sediment comprising a specific surface.

Critical shear stresses were calculated for several alluvial deposits by using dimensionless critical shear stress values, or Shields τ^*_c, of 0.030 and 0.045 because a precise τ^*_c value for each sediment deposit could not be determined. A peak discharge of 9,470 ft^3/s in 1995 and onsite observations and photographs in 1994 and 1995 confirmed sediment entrainment or reworking on several geomorphic surfaces inundated by the peak discharge. Physical evidence of sediment entrainment, or absence of sediment entrainment, on inundated sediment-measurement sites generally was consistent with critical shear stresses estimated with τ^*_c of 0.030 in the Warner Point study reach; however, a preferred τ^*_c could not be determined for the debris-fan distal margin in the Red Rock Canyon study reach. A τ^*_c value other than 0.030 could be appropriate for some geomorphic surfaces in the study reach; however, determination of τ^*_c, such as by the method of Andrews (1983), could not be made in this study.

Entrainment potential over a range of discharges can be summarized by the ratio of boundary shear stress to the critical shear stress (τ_o/τ_c), given local hydraulic geometry and sediment-size characteristics. Differing entrainment potential for similar geomorphic surfaces (low-flow banks, low-elevation bars, high-elevation bars, and so forth) indicates that estimation of minimum streamflow requirements based on sediment mobility require site-specific geomorphic and sedimentologic data.

REFERENCES CITED

Andrews, E.D., 1983, Entrainment of gravel from naturally sorted riverbed material: Geological Society of America Bulletin, v. 94, p. 1225–1231.

Arcement, G.J., and Schneider, V.R., 1989, Guide for selecting Manning's roughness coefficients for natural channels and flood plains: U.S. Geological Survey Water-Supply Paper 2339, 38 p.

Barnes, H.H., Jr., 1967, Roughness characteristics of natural channels: U.S. Geological Survey Water-Supply Paper 1849, 213 p.

Carling, P.A., 1983, Threshold of coarse sediment transport in broad and narrow natural streams: Earth Surface Processes, v. 8, p. 1–18.

Chow, V.T., 1959, Open-channel hydraulics: New York, McGraw-Hill, Inc., 680 p.

Elliott, J.G., and Hammack, L.A., in press, Entrainment of riparian gravel and cobbles in an alluvial reach of a regulated canyon river: Regulated Rivers—Research and Management.

Elliott, J.G., and Parker, R.S., 1992, Potential climate-change effects on bed-material entrainment, the Gunnison Gorge, Colorado, *in* Hermann, Raymond, ed., Managing water resources during global change: Proceedings, American Water Resources Association, 28th Annual Conference and Symposia, Reno, Nevada, November 1–5, 1992, p. 751–759.

Elliott, J.G., and Parker, R.S., 1997, Altered streamflow and sediment entrainment in the Gunnison Gorge: Journal of the American Water Resources Association, v. 33, no. 5, October 1997, p. 1041–1054.

Fahnestock, R.K., 1963, Morphology and hydrology of a glacial stream—White River, Mount Rainier, Washington: U.S. Geological Survey Professional Paper 442–A, p. 1–70.

Friedman, J.M., and Auble, G.T., in press, Mortality of riparian box elder from sediment mobilization and extended inundation: Regulated Rivers—Research and Management.

Hansen, W.R., 1965, The Black Canyon of the Gunnison today and yesterday: U.S. Geological Survey Bulletin 1191, 76 p.

Hydrologic Engineering Center, 1990, HEC-2 Water surface profiles—Program user's manual: U.S. Army Corps of Engineers, 47 p.

Hydrologic Engineering Center, 1997, HEC-RAS River analysis system—Program user's manual, Version 2.0: U.S. Army Corps of Engineers, variously paged.

Komar, P.D., 1987, Selective gravel entrainment and the empirical evaluation of flow competence: Sedimentology, v. 34, p. 1165–1176.

Lane, E.W., 1955, Design of stable channels: Transactions, American Society of Civil Engineers, v. 120, no. 2776, p. 1234–1279.

Lisle, T.E., Iseya, F., and Ikeda, H., 1993, Response of a channel with alternate bars to a decrease in supply of mixed-size bed load—A flume experiment: Water Resources Research v. 29, no. 11, p. 3623–3629.

Milhous, R.T., 1982, Effect of sediment transport and flow regulation on the ecology of gravel-bed rivers, *in* Hey, R.D., Bathhurst, J.C., and Thorne, C.R., eds., Gravel-bed rivers: Chichester, England, John Wiley and Sons, Limited, p. 819–842.

Neill, C.R., 1968, A re-examination of the beginning of movement for coarse granular bed materials: Wallingford, United Kingdom, Hydraulics Research Station, Report No. INT 68, 37 p.

Parker, Gary, Klingman, P.C., and McLean, D.G., 1982, Bedload and size distribution in paved gravel-bed streams: American Society of Civil Engineers, Journal of the Hydraulics Division 108(HY4) p. 544–571.

Powell, D.M., and Ashworth, P.J., 1995, Spatial pattern of flow competence and bed load transport in a divided gravel bed river: Water Resources Research, v. 31, no. 3, p. 741–752.

Shields, A., 1936, Application of similarity principles and turbulence research to bedload movement, *translated from* Anwendung der Aehnlichkeitsmechanik und der Turbulenzforschung auf die Geschiebewegung: Mitteilung Preussischen Versuchanstalt für Wasserbau und Schiffbau, Berlin, No. 26, by W.P. Ott and J.C. van Uchelen, California Institute of Technology Hydrodynamics, Pasadena, California, Report No. 167, 43 p.

U.S. Interagency Advisory Committee on Water Data, 1982, Guidelines for determining flood-flow frequency, Bulletin 17B of the Hydrology Subcommittee: Reston, Va., U.S. Geological Survey, Office of Water Data Coordination, 183 p.

Warner, M.T., and Walker, D.B., 1972, Through the Black Canyon: Ann Arbor, Michigan, Braun-Brumfield, Inc., 45 p.

Webb, R.H., 1996, Grand Canyon, a century of environmental change—Rephotography of the 1889–1890 Stanton Expedition: Tucson, University of Arizona Press, 290 p.

Webb, R.H., Melis, T.S., Wise, T.W., and Elliott, J.G., 1996, The great cataract—Effects of late Holocene debris flows on Lava Falls Rapid, Grand Canyon National Park and Hualapai Indian Reservation, Arizona: U.S. Geological Survey Open-File Report 96–460, 96 p.

Wilcock, P.R., 1992, Flow competence—A criticism of a classic concept: Earth Surface Processes and Landforms, v. 17, p. 289–298.

Wilcock, P.R., and McArdell, B.W., 1993, Surface-based fractional transport rates—Mobilization thresholds and partial transport of a sand-gravel sediment: Water Resources Research v. 29, no. 4, p. 1297–1312.

Wolman, M.G., 1954, A method of sampling coarse river-bed material: American Geophysical Union Transactions v. 35, p. 951–956.

APPENDIX

A

Figure 10. Replicate photographs of the Warner Point study reach from monument 0011-A, downstream view of Bar 8.2L near cross section V5: (*A*) August 3, 1994, 420 cubic feet per second, (*B*) September 25, 1995, 610 cubic feet per second.

B

Figure 10. Replicate photographs of the Warner Point study reach from monument 0011-A, downstream view of Bar 8.2L near cross section V5: (*A*) August 3, 1994, 420 cubic feet per second, (*B*) September 25, 1995, 610 cubic feet per second—Continued.

A

Figure 11. Replicate photographs of the Warner Point study reach from monument 0020-B, downstream view of Bar 8.5R near cross section H3: (*A*) August 3, 1994, 425 cubic feet per second, (*B*) September 25, 1995, 580 cubic feet per second.

B

Figure 11. Replicate photographs of the Warner Point study reach from monument 0020-B, downstream view of Bar 8.5R near cross section H3: (*A*) August 3, 1994, 425 cubic feet per second, (*B*) September 25, 1995, 580 cubic feet per second—Continued.

A

Figure 12. Replicate photographs of the Warner Point study reach from monument 0021-A, upstream view of Bar 8.5R near cross section H3: (*A*) August 3, 1994, 425 cubic feet per second, (*B*) September 25, 1995, 580 cubic feet per second.

B

Figure 12. Replicate photographs of the Warner Point study reach from monument 0021-A, upstream view of Bar 8.5R near cross section H3: (*A*) August 3, 1994, 425 cubic feet per second, (*B*) September 25, 1995, 580 cubic feet per second—Continued.

A

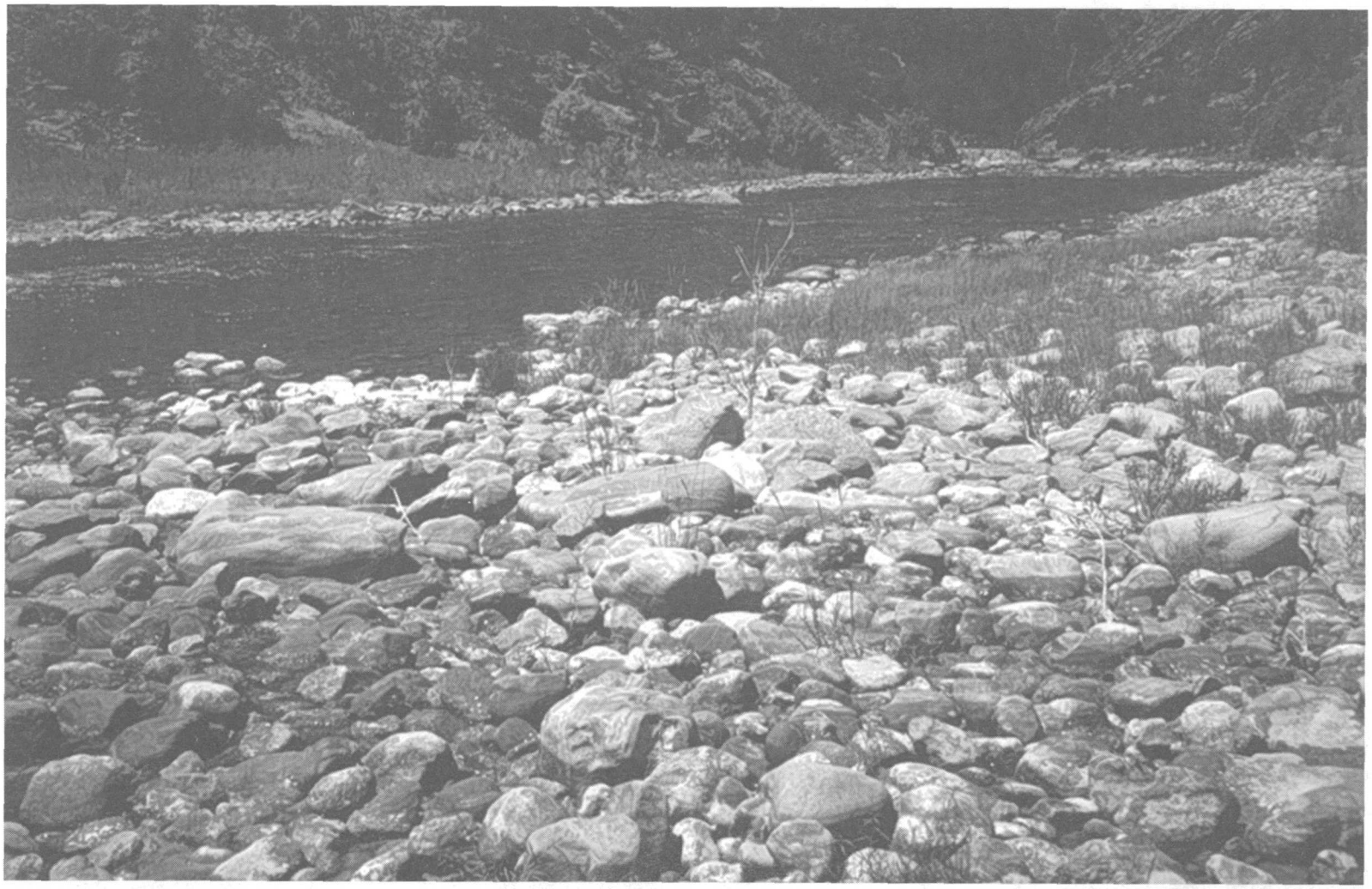

Figure 13. Replicate photographs of the Warner Point study reach from monument 0021-D, downstream view of Bar 8.5R near cross section H60: (*A*) August 3, 1994, 425 cubic feet per second, (*B*) September 25, 1995, 580 cubic feet per second.

B

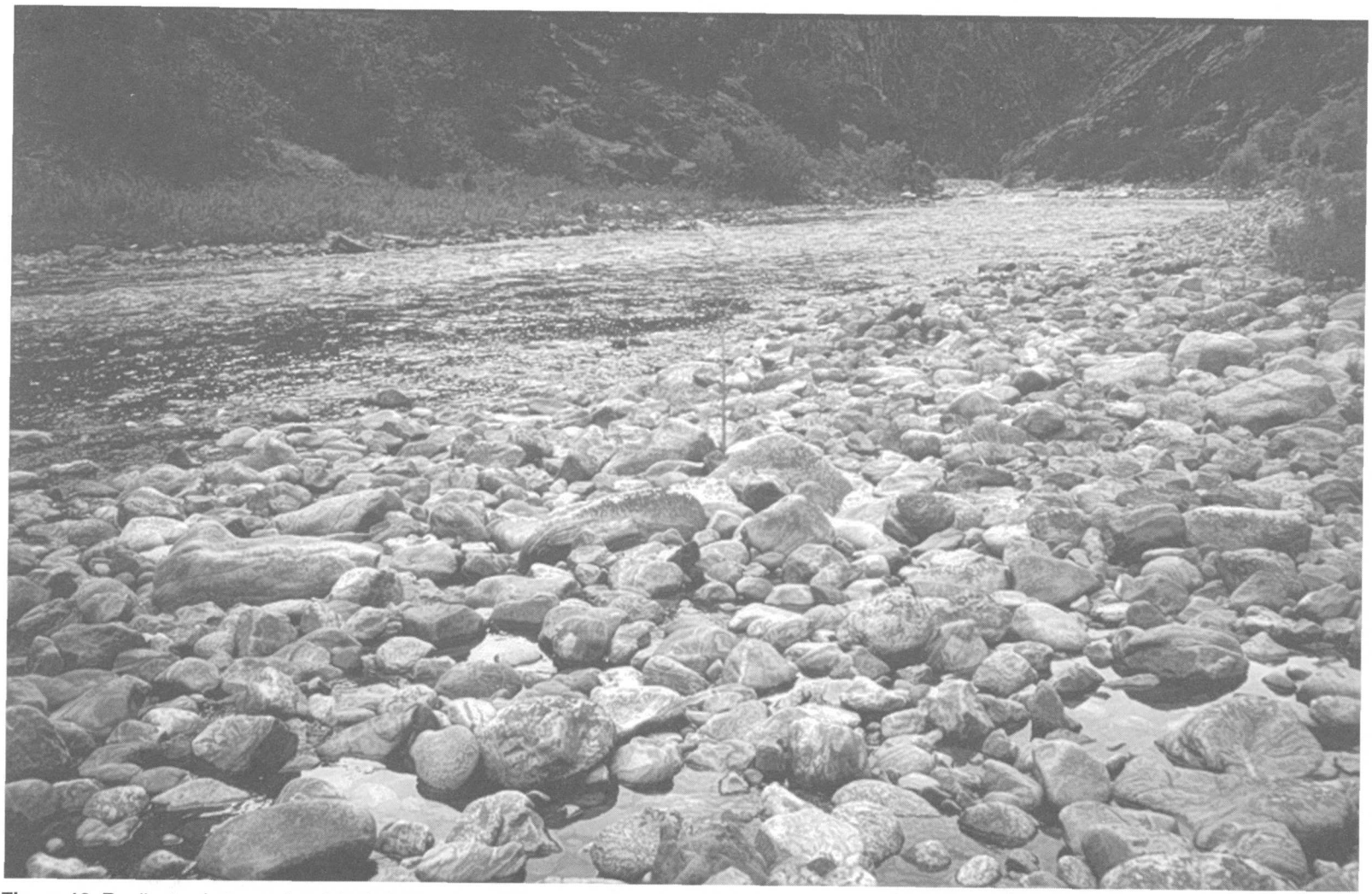

Figure 13. Replicate photographs of the Warner Point study reach from monument 0021-D, downstream view of Bar 8.5R near cross section H60: (A) August 3, 1994, 425 cubic feet per second, (B) September 25, 1995, 580 cubic feet per second—Continued.

A

Figure 14. Replicate photographs of the Red Rock Canyon study reach from monument 0003-B2, cross-channel view of bar near cross section G1: (*A*) August 5, 1994, 400 cubic feet per second, (*B*) September 26, 1995, 600 cubic feet per second.

B

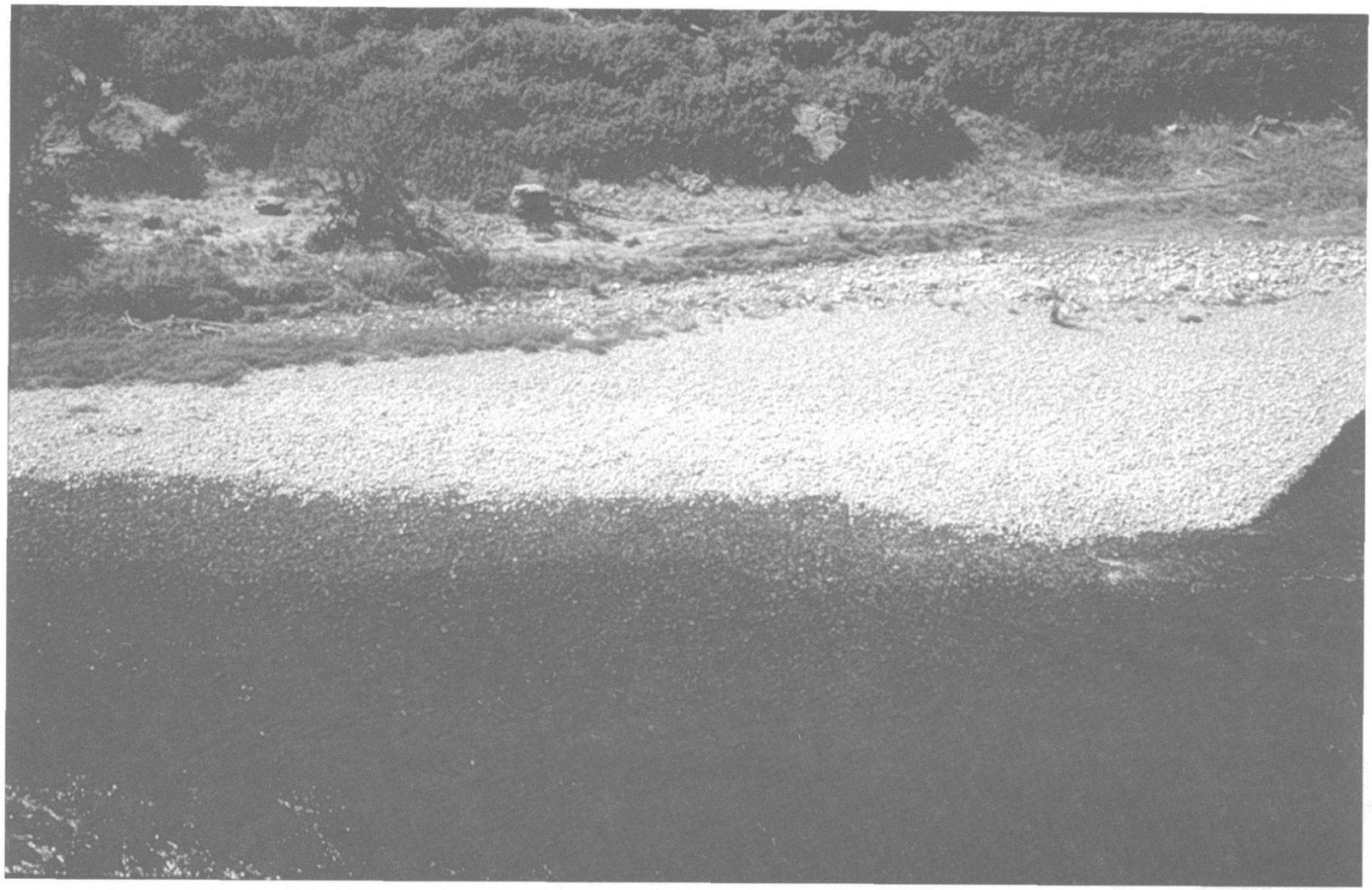

Figure 14. Replicate photographs of the Red Rock Canyon study reach from monument 0003-B2, cross-channel view of bar near cross section G1: (*A*) August 5, 1994, 400 cubic feet per second, (*B*) September 26, 1995, 600 cubic feet per second—Continued.

A

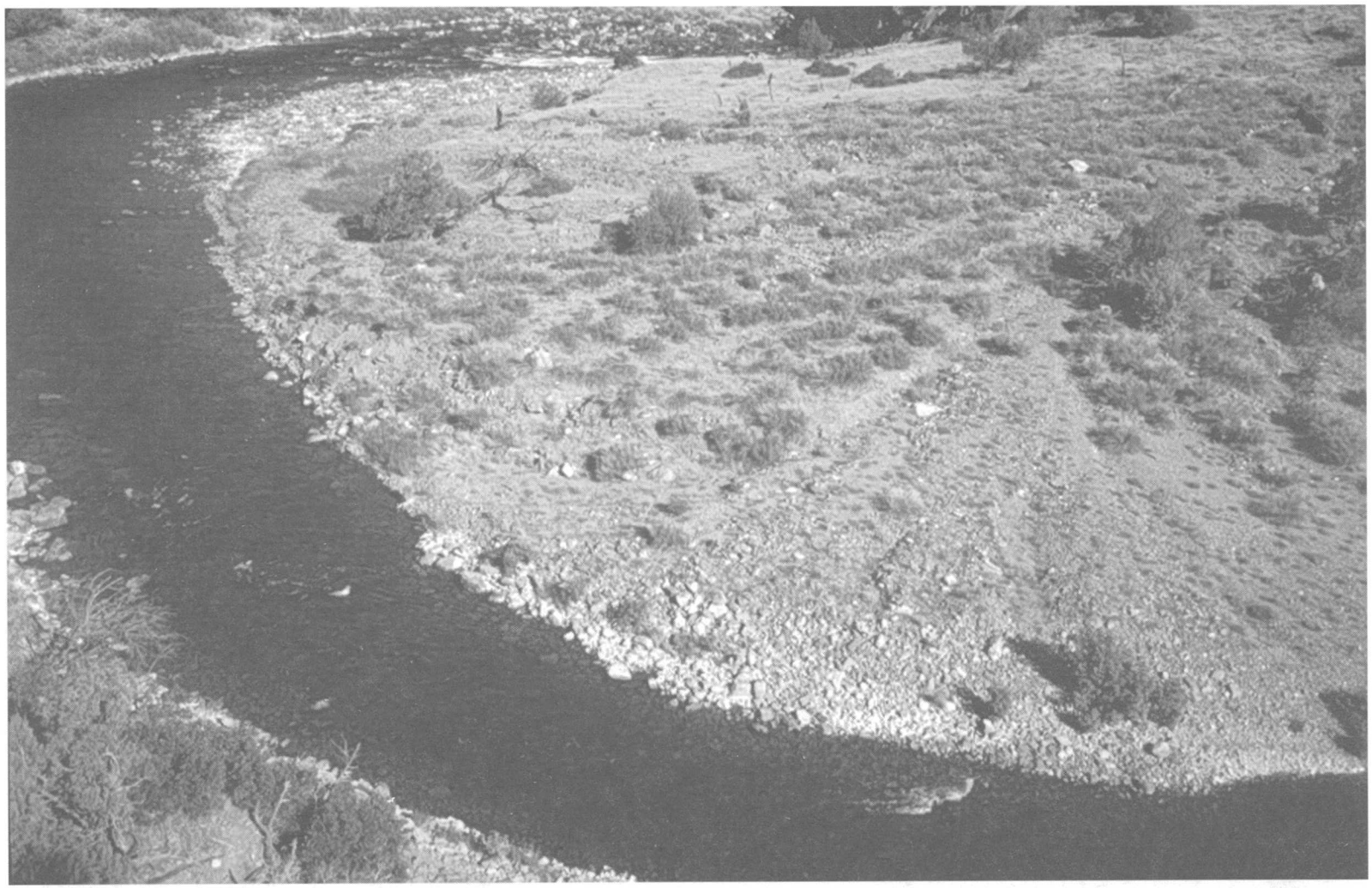

Figure 15. Replicate photographs of the Red Rock Canyon study reach from monument 0005-D, downstream view of debris fan at Tributary 11.3R: (*A*) August 6, 1994, 400 cubic feet per second, (*B*) September 26, 1995, 600 cubic feet per second.

B

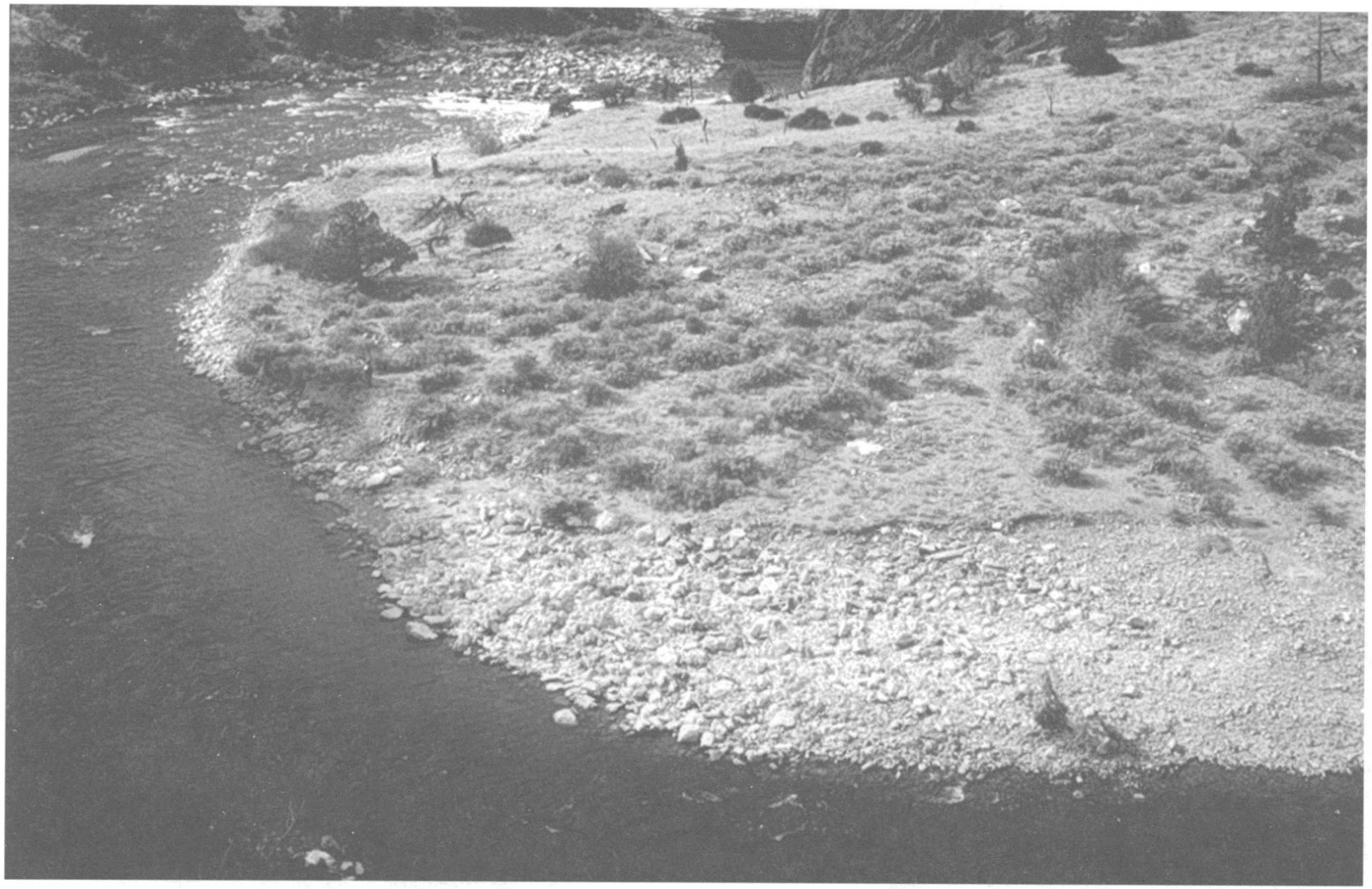

Figure 15. Replicate photographs of the Red Rock Canyon study reach from monument 0005-D, downstream view of debris fan at Tributary 11.3R: (*A*) August 6, 1994, 400 cubic feet per second, (*B*) September 26, 1995, 600 cubic feet per second—Continued.

A

Figure 16. Replicate photographs of the Red Rock Canyon study reach from monument 0006-B, downstream view of bar above cross section H2: (*A*) August 6, 1994, 400 cubic feet per second, (*B*) September 26, 1995, 600 cubic feet per second.

B

Figure 16. Replicate photographs of the Red Rock Canyon study reach from monument 0006-B, downstream view of bar above cross section H2: (*A*) August 6, 1994, 400 cubic feet per second, (*B*) September 26, 1995, 600 cubic feet per second—Continued.

A

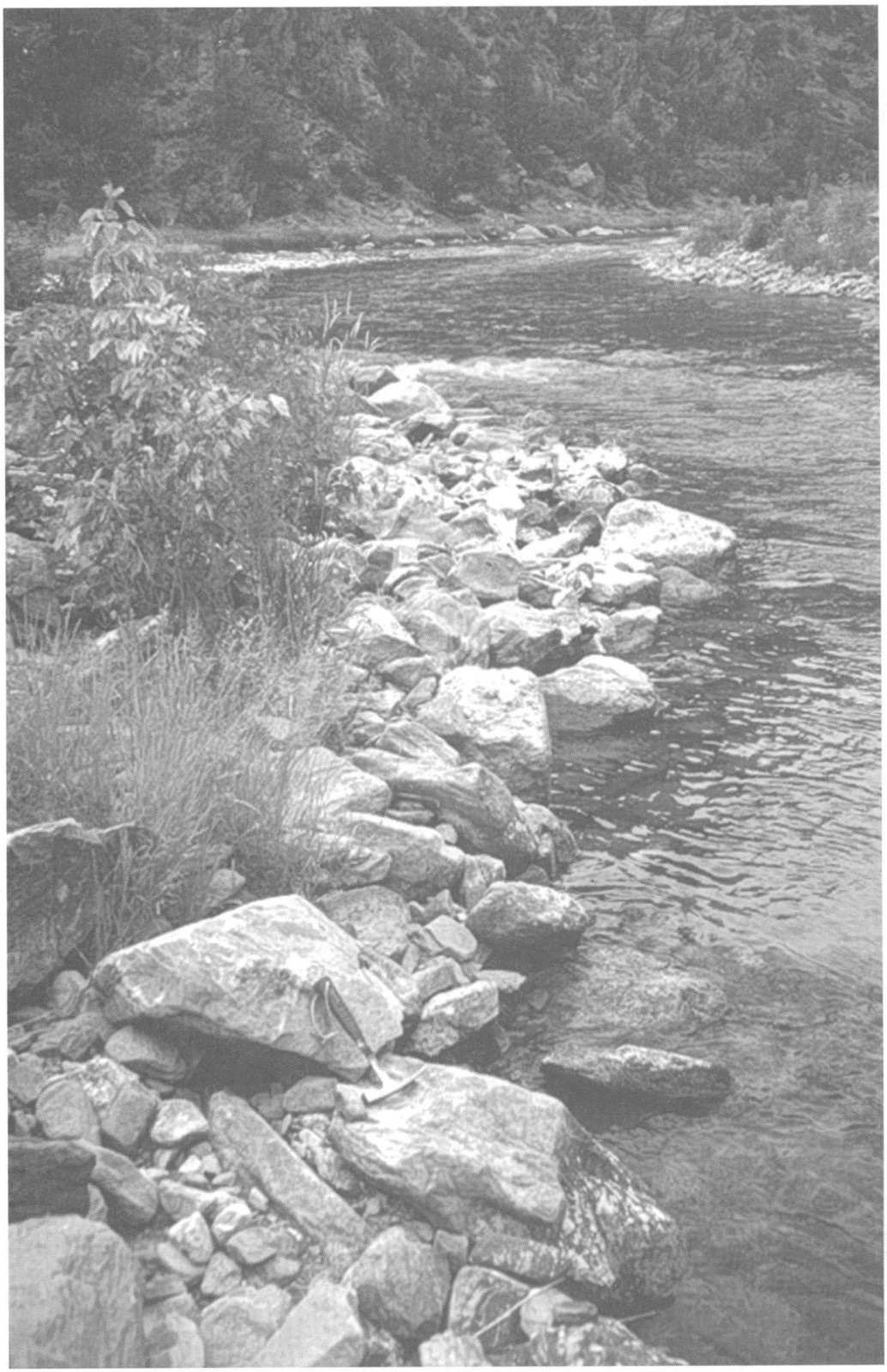

Figure 17. Replicate photographs of the Red Rock Canyon study reach from monument 0010-U, upstream view of debris-fan distal margin near cross section H1: (*A*) August 8, 1994, 410 cubic feet per second, (*B*) September 26, 1995, 600 cubic feet per second.

B

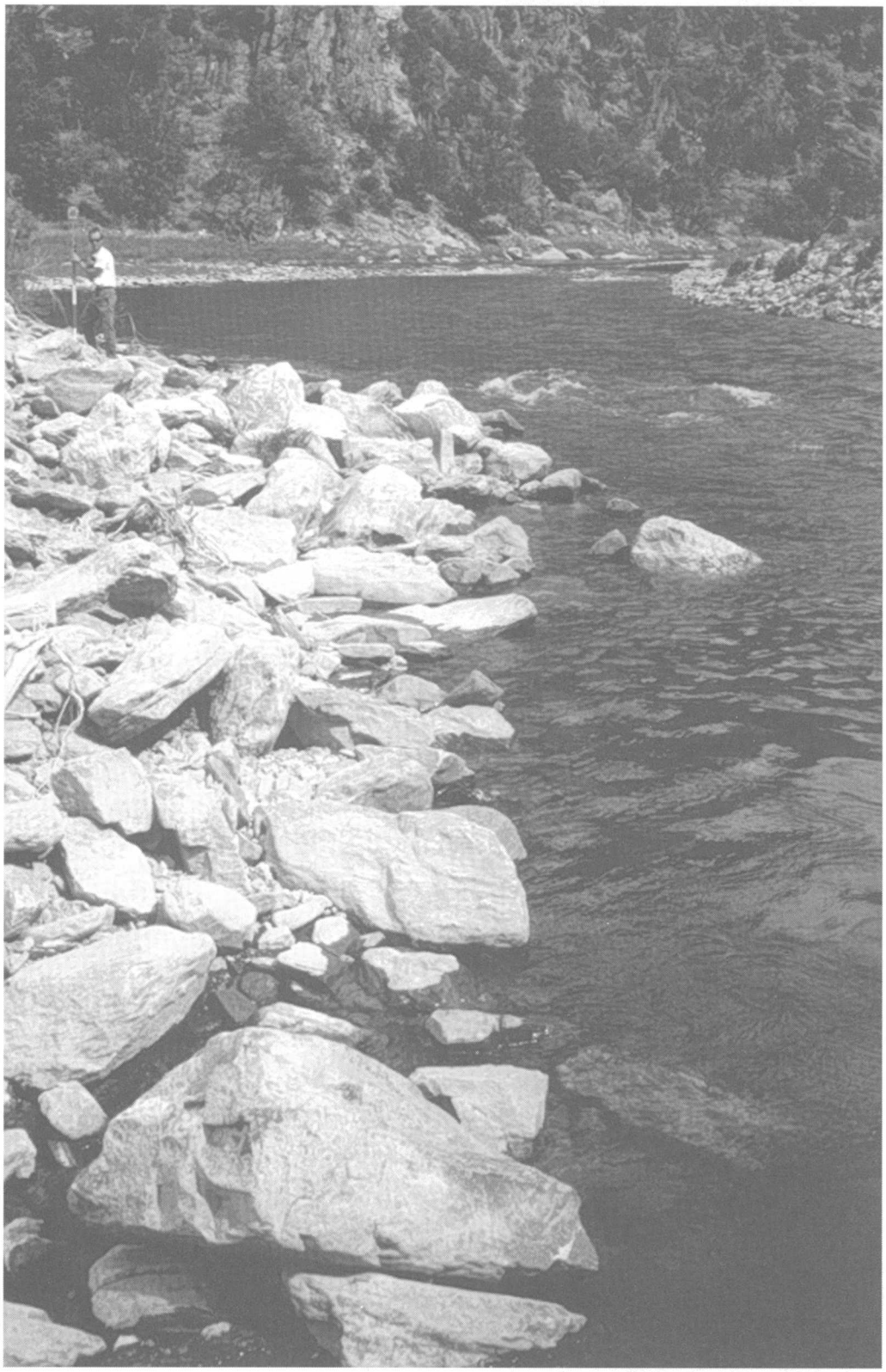

Figure 17. Replicate photographs of the Red Rock Canyon study reach from monument 0010-U, upstream view of debris-fan distal margin near cross section H1: (*A*) August 8, 1994, 410 cubic feet per second, (*B*) September 26, 1995, 600 cubic feet per second—Continued.

A

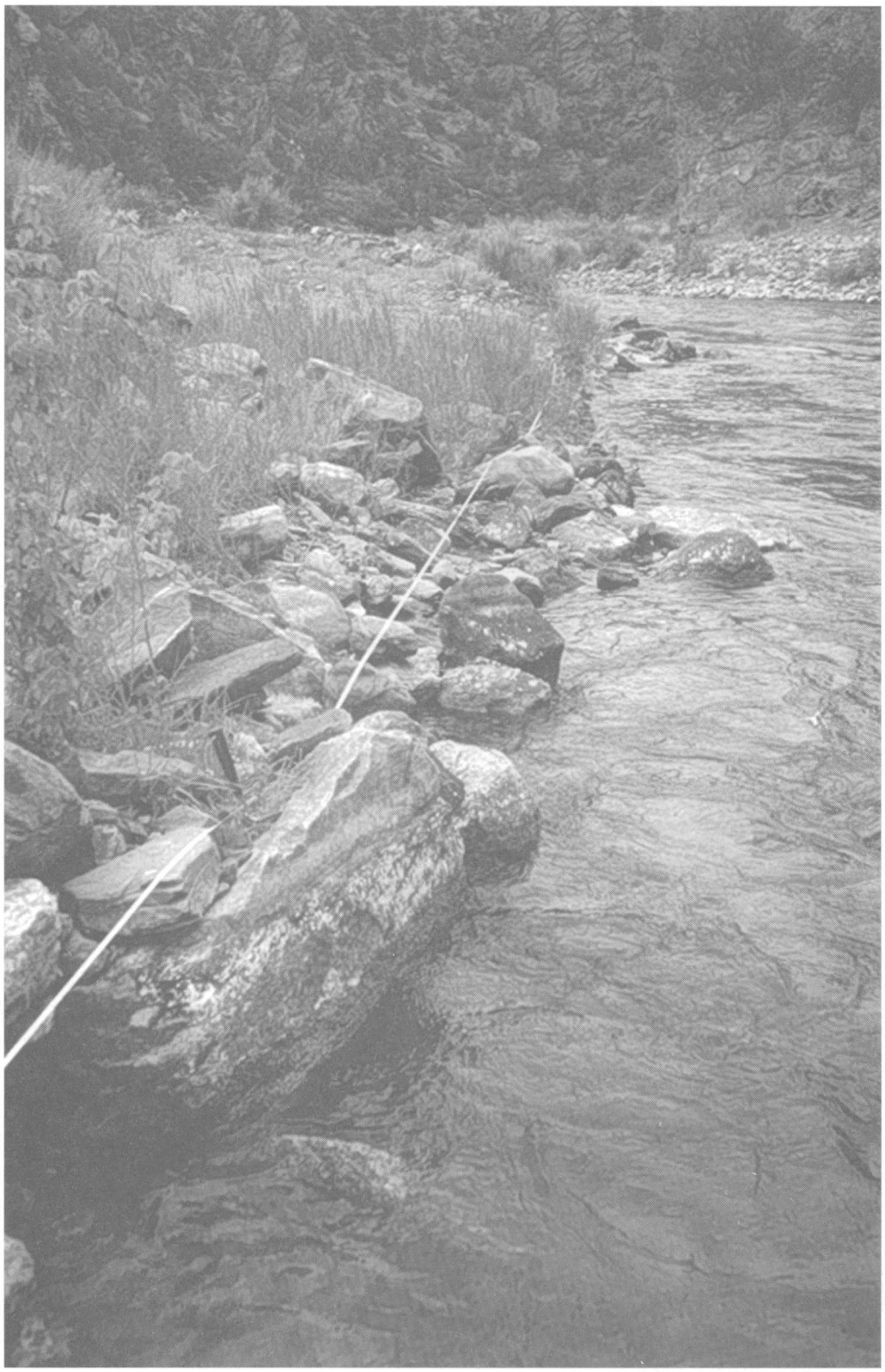

Figure 18. Replicate photographs of the Red Rock Canyon study reach from monument 0011-U, upstream view of debris-fan distal margin near cross section F1: (*A*) August 8, 1994, 410 cubic feet per second, (*B*) September 26, 1995, 600 cubic feet per second.

B

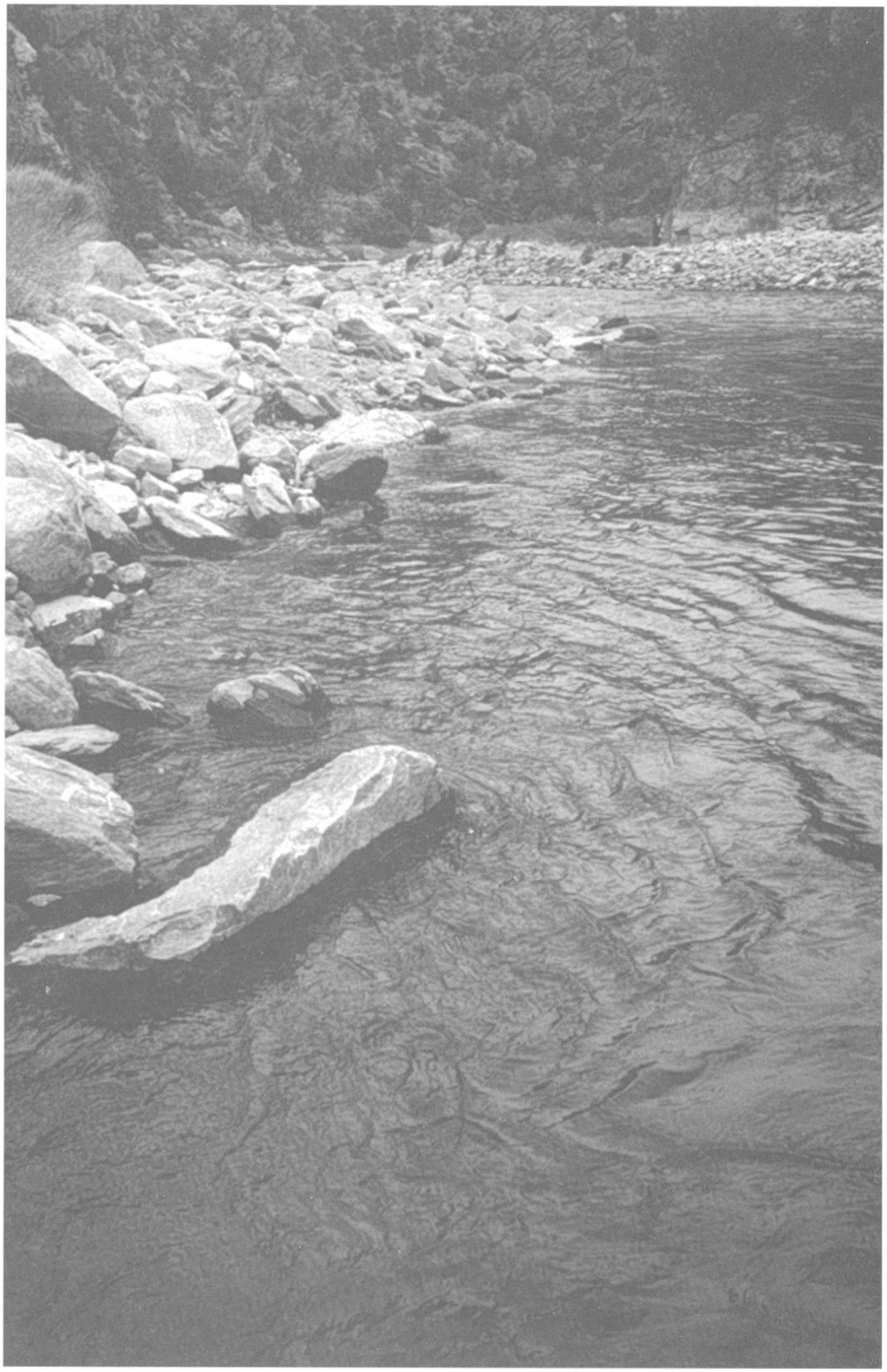

Figure 18. Replicate photographs of the Red Rock Canyon study reach from monument 0011-U, upstream view of debris-fan distal margin near cross section F1: (*A*) August 8, 1994, 410 cubic feet per second, (*B*) September 26, 1995, 600 cubic feet per second—Continued.

☆ U.S. GOVERNMENT PRINTING OFFICE: 1999 — 573-082 / 20079 Region No. 8

USGS/WRIR 99-4082